



GE Energy

Proprietary Notice

*This letter forwards GNF  
proprietary information in  
accordance with 10CFR2.390.  
Upon the removal of Enclosure 1,  
the balance of this letter may be  
considered non-proprietary.*

David H. Hinds  
Manager, ESBWR

PO Box 780 M/C L60  
Wilmington, NC 28402-0780  
USA

T 910 675 6363  
F 910 362 6363  
david.hinds@ge.com

MFN 06-297

Docket No. 52-010

August 23, 2006

U.S. Nuclear Regulatory Commission  
Document Control Desk  
Washington, D.C. 20555-0001

**Subject: Response to Portion of NRC Request for Additional Information  
Letter No. 53 Related to ESBWR Design Certification Application –  
DCD Chapter 4 and GNF Topical Reports – RAI Numbers 4.2-2  
through 4.2-7, 4.3-3, 4.3-4, 4.4-2, 4.4-5, 4.4-6, 4.4-15 through 4.4-17,  
4.4-19, 4.4-24, 4.4-27, 4.4-31 through 4.4-34, 4.4-36, through 4.4-38,  
4.4-42 through 4.4-50, 4.4-52 through 4.4-56, 4.8-1 through 4.8-16**

Enclosure 1 contains GE's response to the subject NRC RAIs transmitted via the  
Reference 1 letter.

Enclosure 1 contains GNF proprietary information as defined by 10 CFR 2.390. GNF  
customarily maintains this information in confidence and withholds it from public  
disclosure. A non proprietary version is provided in Enclosure 2.

The affidavit contained in Enclosure 3 identifies that the information contained in  
Enclosure 1 has been handled and classified as proprietary to GNF. GE hereby requests  
that the information of Enclosure 1 be withheld from public disclosure in accordance  
with the provisions of 10 CFR 2.390 and 9.17.

DA08

If you have any questions about the information provided here, please let me know.

Sincerely,



David H. Hinds  
Manager, ESBWR

Enclosures:

1. MFN 06-297 - Response to Portion of NRC Request for Additional Information Letter No. 53 Related to ESBWR Design Certification Application – DCD Chapter 4 and GNF Topical Reports – RAI Numbers 4.2-2 through 4.2-7, 4.3-3, 4.3-4, 4.4-2, 4.4-5, 4.4-6, 4.4-15 through 4.4-17, 4.4-19, 4.4-24, 4.4-27, 4.4-31 through 4.4-34, 4.4-36, through 4.4-38, 4.4-42 through 4.4-50, 4.4-52 through 4.4-56, 4.8-1 through 4.8-16 – GNF Proprietary Information
2. MFN 06-297 - Response to Portion of NRC Request for Additional Information Letter No. 53 Related to ESBWR Design Certification Application – DCD Chapter 4 and GNF Topical Reports – RAI Numbers 4.2-2 through 4.2-7, 4.3-3, 4.3-4, 4.4-2, 4.4-5, 4.4-6, 4.4-15 through 4.4-17, 4.4-19, 4.4-24, 4.4-27, 4.4-31 through 4.4-34, 4.4-36, through 4.4-38, 4.4-42 through 4.4-50, 4.4-52 through 4.4-56, 4.8-1 through 4.8-16 – Non Proprietary Version
3. Affidavit – Jens G. M. Andersen – dated August 23, 2006

Reference:

1. MFN 06-288, Letter from U. S. Nuclear Regulatory Commission to Mr. David H. Hinds, *Request for Additional Information Letter No. 53 Related to ESBWR Design Certification Application*, August 16, 2006

cc: WD Beckner USNRC (w/o enclosures)  
AE Cabbage USNRC (with enclosures)  
LA Dudes USNRC (w/o enclosures)  
AA Lingenfelter GNF/Wilmington (w/o enclosures)  
GB Stramback GE/San Jose (with enclosures)  
eDRFs 53-7116, 56-0271, 56-0274, 56-0275, 56-0276, 56-0277, 56-4527, 56-5590, 56-7094,  
56-7102, 56-7217, 56-8456, 56-8821, 56-9169, 56-9170, 57-0871, 57-1359, 57-1360,  
57-2098, 57-2106, 57-2336, 57-2412, 57-2476, 57-2692, 57-2701, 57-2705, 57-2708,  
57-2773, 57-2870, 57-3593, 57-3633

**ENCLOSURE 3**

**MFN 06-297**

**Affidavit**

## Affidavit

I, Jens G. M. Andersen, state as follows:

- (1) I am Consulting Engineer, Thermal Hydraulic Methods, Global Nuclear Fuel – Americas, L.L.C. (“GNF-A”) and have been delegated the function of reviewing the information described in paragraph (2) which is sought to be withheld, and have been authorized to apply for its withholding.
- (2) The information sought to be withheld is contained in Enclosure 1 of GE letter MFN 06-297, David H. Hinds to U. S. Nuclear Regulatory Commission, *Response to Portion of NRC Request for Additional Information Letter No. 53 Related to ESBWR Design Certification Application – DCD Chapter 4 and GNF Topical Reports – RAI Numbers 4.2-2 through 4.2-7, 4.3-3, 4.3-4, 4.4-2, 4.4-5, 4.4-6, 4.4-15 through 4.4-17, 4.4-19, 4.4-24, 4.4-27, 4.4-31 through 4.4-34, 4.4-36, through 4.4-38, 4.4-42 through 4.4-50, 4.4-52 through 4.4-56, 4.8-1 through 4.8-16*, dated August 23, 2006. The proprietary information in Enclosure 1, *Response to Portion of NRC Request for Additional Information Letter No. 53 Related to ESBWR Design Certification Application – DCD Chapter 4 and GNF Topical Reports – RAI Numbers 4.2-2 through 4.2-7, 4.3-3, 4.3-4, 4.4-2, 4.4-5, 4.4-6, 4.4-15 through 4.4-17, 4.4-19, 4.4-24, 4.4-27, 4.4-31 through 4.4-34, 4.4-36, through 4.4-38, 4.4-42 through 4.4-50, 4.4-52 through 4.4-56, 4.8-1 through 4.8-16 – GNF Proprietary Information*, is delineated by double underlined dark red font text and is enclosed inside double square brackets. Figures and large equation objects are identified with double square brackets before and after the object. The superscript notation<sup>(3)</sup> refers to Paragraph (3) of this affidavit, which provides the basis for the proprietary determination.
- (3) In making this application for withholding of proprietary information of which it is the owner or licensee, GNF-A relies upon the exemption from disclosure set forth in the Freedom of Information Act (“FOIA”), 5 USC Sec. 552(b)(4), and the Trade Secrets Act, 18 USC Sec. 1905, and NRC regulations 10 CFR 9.17(a)(4) and 2.390(a)(4) for “trade secrets” (Exemption 4). The material for which exemption from disclosure is here sought also qualify under the narrower definition of “trade secret,” within the meanings assigned to those terms for purposes of FOIA Exemption 4 in, respectively, Critical Mass Energy Project v. Nuclear Regulatory Commission, 975F2d871 (DC Cir. 1992), and Public Citizen Health Research Group v. FDA, 704F2d1280 (DC Cir. 1983).
- (4) Some examples of categories of information which fit into the definition of proprietary information are:
  - a. Information that discloses a process, method, or apparatus, including supporting data and analyses, where prevention of its use by GNF-A’s competitors without license from GNF-A constitutes a competitive economic advantage over other companies;

- b. Information which, if used by a competitor, would reduce his expenditure of resources or improve his competitive position in the design, manufacture, shipment, installation, assurance of quality, or licensing of a similar product;
- c. Information which reveals aspects of past, present, or future GNF-A customer-funded development plans and programs, of potential commercial value to GNF-A;
- d. Information which discloses patentable subject matter for which it may be desirable to obtain patent protection.

The information sought to be withheld is considered to be proprietary for the reasons set forth in paragraphs (4)a. and (4)b., above.

- (5) To address the 10 CFR 2.390 (b) (4), the information sought to be withheld is being submitted to NRC in confidence. The information is of a sort customarily held in confidence by GNF-A, and is in fact so held. Its initial designation as proprietary information, and the subsequent steps taken to prevent its unauthorized disclosure, are as set forth in (6) and (7) following. The information sought to be withheld has, to the best of my knowledge and belief, consistently been held in confidence by GNF-A, no public disclosure has been made, and it is not available in public sources. All disclosures to third parties including any required transmittals to NRC, have been made, or must be made, pursuant to regulatory provisions or proprietary agreements which provide for maintenance of the information in confidence.
- (6) Initial approval of proprietary treatment of a document is made by the manager of the originating component, the person most likely to be acquainted with the value and sensitivity of the information in relation to industry knowledge, or subject to the terms under which it was licensed to GNF-A. Access to such documents within GNF-A is limited on a "need to know" basis.
- (7) The procedure for approval of external release of such a document typically requires review by the staff manager, project manager, principal scientist or other equivalent authority, by the manager of the cognizant marketing function (or his delegate), and by the Legal Operation, for technical content, competitive effect, and determination of the accuracy of the proprietary designation. Disclosures outside GNF-A are limited to regulatory bodies, customers, and potential customers, and their agents, suppliers, and licensees, and others with a legitimate need for the information, and then only in accordance with appropriate regulatory provisions or proprietary agreements.
- (8) The information identified in paragraph (2) is classified as proprietary because it contains details of GNF-A's fuel design and licensing methodology.

The development of the methods used in these analyses, along with the testing, development and approval of the supporting methodology was achieved at a significant cost, on the order of several million dollars, to GNF-A or its licensor.

- (9) Public disclosure of the information sought to be withheld is likely to cause substantial harm to GNF-A's competitive position and foreclose or reduce the availability of profit-making opportunities. The fuel design and licensing methodology is part of GNF-A's comprehensive BWR safety and technology base, and its commercial value extends beyond the original development cost. The value of the technology base goes beyond the extensive physical database and analytical methodology and includes development of the expertise to determine and apply the appropriate evaluation process. In addition, the technology base includes the value derived from providing analyses done with NRC-approved methods.

The research, development, engineering, analytical, and NRC review costs comprise a substantial investment of time and money by GNF-A or its licensor.

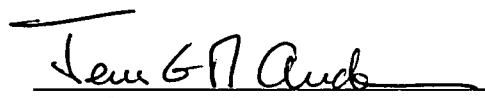
The precise value of the expertise to devise an evaluation process and apply the correct analytical methodology is difficult to quantify, but it clearly is substantial.

GNF-A's competitive advantage will be lost if its competitors are able to use the results of the GNF-A experience to normalize or verify their own process or if they are able to claim an equivalent understanding by demonstrating that they can arrive at the same or similar conclusions.

The value of this information to GNF-A would be lost if the information were disclosed to the public. Making such information available to competitors without their having been required to undertake a similar expenditure of resources would unfairly provide competitors with a windfall, and deprive GNF-A of the opportunity to exercise its competitive advantage to seek an adequate return on its large investment in developing and obtaining these very valuable analytical tools.

I declare under penalty of perjury that the foregoing affidavit and the matters stated therein are true and correct to the best of my knowledge, information, and belief.

Executed at Wilmington, North Carolina this 23<sup>rd</sup> day of August 2006.

  
Jens G. M. Andersen  
Global Nuclear Fuels – Americas, LLC

## **ENCLOSURE 2**

**MFN 06-297**

**Response to Portion of NRC Request for**

**Additional Information Letter No. 53**

**Related to ESBWR Design Certification Application**

**DCD Chapter 4 and GNF Topical Reports**

**RAI Numbers 4.2-2 through 4.2-7, 4.3-3, 4.3-4, 4.4-2, 4.4-5, 4.4-6,  
4.4-15 through 4.4-17, 4.4-19, 4.4-24, 4.4-27, 4.4-31 through 4.4-34,  
4.4-36, through 4.4-38, 4.4-42 through 4.4-50, 4.4-52 through 4.4-56,  
4.8-1 through 4.8-16**

**Non Proprietary Version**

NRC RAI 4.2-2

*DCD Tier 2, Section 4.2.1.1.4 states, "The oxide thickness itself is not separately limiting and no design limit on cladding oxide thickness is therefore specified." (Similar statement for hydrogen content in Section 4.2.1.1.5.)*

*(a) Describe the extent of the irradiated and unirradiated mechanical testing database for both fuel rods and assembly components (including channels) with respect to oxide and hydride concentrations and orientations used to support the thermal-mechanical analyses.*

*(b) Demonstrate that the cladding is capable of achieving [[  
]] up to expected oxide/hydride concentrations at end-of-life.*

NRC RAI 4.2-4

*DCD Tier 2, Section 4.2.1.1.5 states' "Mechanical properties testing demonstrates that the cladding mechanical properties are negligibly affected for hydrogen contents far in excess of that experienced during normal operation." Provide the mechanical properties testing database, along with pool-side corrosion measurements, to support this statement.*

GE Response

***Combined Response***

GNF recognizes the importance of addressing the effects of Zircaloy component corrosion and corresponding Zircaloy component hydrogen pickup. For the fuel rod cladding, the effects addressed include (1) the heat transfer resistance provided by the cladding oxide thickness, thereby increasing cladding and fuel pellet temperatures, (2) the metal loss as a result of the corrosion reaction, thereby reducing the cladding load carrying ability, and (3) the reduction in cladding material strain capability with sufficiently elevated hydrogen concentration. However, it is GNF's position that so long as those effects are appropriately addressed, no separate limits are required on the Zircaloy oxide thickness and hydrogen content. This approach has enabled the successful development and reliable application of over 14 separate GNF fuel product lines over a period of more than 35 years, and is expected to enable similar reliable performance of the GE14E fuel design for the ESBWR.

GNF performs poolside eddy current lift-off measurements to quantitatively assess cladding corrosion performance. Eddy-current lift-off measurements represent the measured distance between the face of the eddy current probe and the cladding oxide-metal interface. The lift-off measurement necessarily includes the combined thicknesses of the cladding oxide and adhering crud (reactor water corrosion product) layers. As such, the lift-off measurements represent an upper bound of the actual cladding oxide thickness. The available poolside eddy current lift-off measurements are presented in Figure 4.2-2-1. Figure 4.2-2-1 presents a time dependent trend of both a nominal lift-off value and an upper 95 lift-off value. The distribution parameters represented by these trend lines are explicitly included in the statistical fuel rod thermal-mechanical design



and licensing analyses. The nominal trend line represents the best estimate value of actual oxide thickness as confirmed by hotcell metallography at current typical end of life conditions (3 2-year cycles in a high power density BWR/4 resulting in a peak rod average exposure of [[ ]]); the bar shown in Figure 4.2-2-1 represents the mean, 5<sup>th</sup> and 95<sup>th</sup> percentiles in cladding oxide thickness as measured by hotcell metallography. The corresponding statistics for the cladding hydrogen content are a mean value of [[ ]], with a 5<sup>th</sup> percentile approaching zero and an upper 95<sup>th</sup> percentile of [[ ]]. Although the oxide thicknesses observed on non-heat transfer surface components, such as the water rod, are similar to those on the cladding, although occurring on two (inner and outer) surfaces, the corresponding hydrogen pickup can be greater. For example, the hydrogen concentration statistics for Zircaloy-2 water rods at the same end of life exposure are a mean of [[ ]], with a 5<sup>th</sup> percentile of [[ ]] and an upper 95<sup>th</sup> percentile of [[ ]].

[[ ]]

]]

Figure 4.2-2-1  
Poolside Eddy-current Lift-Off Measurements for Fuel Rods Irradiated in Commercial BWRs

The effect of irradiation and hydriding on Zircaloy ductility has been assessed both for non-heat transfer surface components and the fuel rod cladding. For the non-heat transfer surface components, Zircaloy-2 water rods were irradiated to a fast neutron fluence of [[ ]] ( $E > 1$  Mev), providing a hydrogen concentration range from [[ ]]. This water rod material represented an earlier fabrication process and was selected to obtain characterization at higher hydrogen contents than are experienced with current modern GNF fuel designs. For the fuel rod cladding, modern Zr-2 cladding irradiated to end of life conditions (3 2-year cycles in a high power density BWR/4) was selected for mechanical properties characterization, providing prototypical cladding hydrogen contents of [[ ]]. Mechanical properties tests were

conducted at room temperature and reactor operating temperature. The testing utilized localized ductility arc and ring-stretch specimens to measure mechanical properties of the cladding and assembly components in the direction of applied loading during operation. Total and uniform elongation measurement results from these tests are plotted as a function of fast fluence and hydrogen content in Figures 4.2-2-2 and 4.2-2-3, respectively. The distribution of hydrides represented the actual component hydride orientation with the exception of some radial hydrides in the fuel rod cladding formed as a result of hydrogen dissolution during transport cask elevated temperature vacuum drying and corresponding radial hydride precipitation during cooling as a result of the cladding tensile stress caused by the fuel rod internal pressure.

The results in Figures 4.2-2-2 and 4.2-2-3 indicate that Zircaloy, either as fuel rod cladding or assembly component (water rod) retains significant ductility, even in the irradiated and hydrided condition. These results support the current [[ ]], strain limit to hydrogen concentrations up to at least [[ ]], and well support the applicability of this property to the actual hydrided condition at EOL of both the fuel rod cladding and Zircaloy assembly components.

On this basis, GNF proposes to maintain the currently approved licensing methodology to address corrosion and hydrogen effects explicitly, without specification of separate oxide thickness and hydrogen concentration limits. GNF will continue to evaluate Zircaloy corrosion and hydriding effects, for example with the future progression to extended exposures, and, if determined appropriate, will update the cladding plastic strain limit as required to reflect the appropriate mechanical properties for the indicated actual hydrogen concentration condition.

No DCD change will be made in response to these RAIs.

[[

]]

Figure 4.2-2-2

Total and Uniform Elongation vs. Fluence for Irradiated Ziracloy-2 tested at 600K

[[

]]

Figure 4.2-2-3

Total and Uniform Elongation vs. Hydrogen Content for Irradiated Ziracloy-2 tested at  
600K

NRC RAI 4.2-3

*DCD Tier 2, Section 4.2.1.1.4 refers to the GSTRM topical report NEDC-31959P (April 1991). Describe the licensing history of GSTRM, including the staff's review and any subsequent changes to the various fuel performance models (e.g. tuning/calibration) within GSTRM, and the pedigree of this unapproved document.*

GE Response

The GSTRM code was submitted to the NRC for review and approval as part of the GESTR-SAFER LOCA methodology in 1981. At that time the code was denoted GESTR-LOCA. The NRC approved GESTR-LOCA in 1984 (Reference 4.2-3.1).

Shortly thereafter, the NRC approved application of the GESTR-LOCA code for fuel rod thermal-mechanical design and licensing analyses in conjunction with a (primarily) statistically based application methodology for these analyses. The thermal-mechanical version of GESTR-LOCA was denoted GESTR-Mechanical (GSTRM). The review and approval is documented in Reference 4.2-3.2. Material provided to support the application methodology is included in References 4.2-3.3 and 4.2-3.4.

The NRC also approved a process whereby the GESTR-Mechanical code could be updated for application to thermal-mechanical design and licensing analyses providing specific pre-determined requirements were met. This Fuel Property and Performance Model Revision Procedure is documented in Reference 4.2-3.5, where the first application of this procedure is documented in 4.2-3.6. Updates made under this approved process include improved thermal conductivity for (U, Gd)O<sub>2</sub> (Reference 4.2-3.6) and inclusion of additive fuel material properties (Reference 4.2-3.7).

NEDC-31959P was prepared to respond to utility requests for details concerning the GSTRM code. This report was not formally transmitted to the NRC. For this reason, DCD Tier 2, Section 4.2.1.1.4 will be revised to refer to Reference 4.2-3.1 below.

References

- 4.2-3.1 GESTR-LOCA – A Model for the Prediction of Fuel Rod Thermal Performance, NEDE-23785-1-PA (Volume 1), June 1984.
- 4.2-3.2 Letter from C. O. Thomas (NRC) to J. S. Charnley (GE), 'Acceptance for Referencing of Licensing Topical Report NEDE-24011-P-A Amendment 7 to Revision 6, GE Standard Application for Reactor Fuel', March 1, 1985.
- 4.2-3.3 Letter, J. S. Charnley (GE) to C. H. Berlinger (NRC), 'GE Presentation on NEDE-24011-P-A Amendment 7', February 7, 1984 (MFN-017-84).
- 4.2-3.4 Letter, J. S. Charnley (GE) to C. O. Thomas (NRC), 'Response to Request Number One for Additional Information on NEDE-24011, Revision 6, Amendment 7, Response to Question 1', April 23, 2004 (MFN-050-84).

- 4.2-3.5 Letter, J. S. Charnely (GE) to C. O. Thomas (NRC), "GE Procedure for Fuel Property and Performance Model Revision", December 14, 1984 (MFN-169-84).
- 4.2-3.6 Letter, J. S. Charnley (GE) to C. O. Thomas (NRC), "Fuel Property and Performance Model Revisions", December 14, 1984 (MFN-170-84-0).
- 4.2-3.7 Letter, J. S. Charnely (GE) to M. W. Hodges (NRC), "Fuel Property and Performance Model Revisions", July 23, 1987 (MFN-170-84-2).

NRC RAI 4.2-5

*DCD Tier 2, Appendix 4B.2 should define the specific Tier 2 and Tier 2\* thermal-mechanical fuel design requirements. These requirements would then be addressed within a separate fuel assembly mechanical design topical report to demonstrate, using approved models and methods, the acceptability of a proposed fuel assembly design to the ESBWR. The specific thermal-mechanical design requirements may be patterned after the standard review plan. The current text appears to be an overview of a fuel design change process and should be removed.*

GE Response

The current Appendix 4B will be revised to remove all of the design process information. Three sections remain in Appendix 4B: 4B.1 Thermal-Mechanical, 4B.2 Nuclear, and 4B.3 Critical Power Correlation. The current Section 4b.2 becomes Section 4B.1. While Appendix 4B is referenced only by Section 4.2, Fuel Design, the change criteria for the nuclear core design, and critical power correlation should also be defined as Tier 2 \* parameters. Thus, Section 4B.2 and 4B.3 provide the appropriate Tier 2\* criteria for core design and critical power correlation changes prior to the plant first achieving full power.

The proposed Appendix 4B is attached.

## 4B. FUEL LICENSING ACCEPTANCE CRITERIA

The fuel licensing acceptance criteria are presented in the following subsections.

### 4B.1 THERMAL-MECHANICAL

The fuel rod thermal-mechanical design criteria to be satisfied for new fuel designs is presented in [Section 3.0 of NEDC-33242P, GE Licensing Topical Report, GE14 for ESBWR Fuel Rod Thermal-Mechanical Design Report (Reference 4B-1)]\*.

### 4B.2 NUCLEAR

*[A negative Doppler reactivity coefficient is maintained for any operating condition.]\** The Doppler reactivity coefficient is of high importance in reactor safety. The Doppler coefficient of the core is a measure of the reactivity change associated with an increase in the absorption of resonance-energy neutrons caused by a change in the temperature of the material and is a function of the average of the bundle Doppler coefficients. A negative Doppler coefficient provides instantaneous negative reactivity feedback to any rise in fuel temperature, on a gross or local basis and thus assures the tendency of self-control.

*[A negative core moderator void reactivity coefficient resulting from boiling in the active flow channels is maintained for any operating conditions.]\** The core moderator void coefficient resulting from boiling in the active flow channels is maintained negative over the complete range of ESBWR operation. This flattens the radial power distribution and provides ease of reactor control due to the negative void feedback mechanism.

*[A negative moderator temperature reactivity coefficient is maintained for temperatures equal to or greater than hot standby.]\** The moderator temperature coefficient is associated with a change in the moderating capability of the water. Once the reactor reaches the power producing range, boiling begins and the moderator temperature remains essentially constant. The moderator temperature reactivity coefficient is negative during power operation.

*[To prevent a super prompt critical reactivity insertion accident originating from any operating condition, the net prompt reactivity feedback due to prompt heating of the moderator and fuel is negative.]\** The mechanical and nuclear designs of the fuel are such that the prompt reactivity feedback (requiring no conductive or convective heat transfer and no operator action) provides an automatic shutdown mechanism in the event of a super prompt reactivity incident. This characteristic ensures rapid termination of super prompt critical accidents, with additional long-term shutdown capability due to negative void coefficient, for those cases where conductive heat transfer from the fuel to the water results in boiling in the active channel region.

*[A negative power reactivity coefficient (as determined by calculating the reactivity change due to an incremental power change from a steady-state base power level) is maintained for all operating power levels above hot standby.]\** A negative power coefficient provides an inherent negative feedback mechanism to provide more reliable control of the plant as the operator performs power maneuvers. It is particularly effective in preventing xenon initiated power oscillations in the core. The power coefficient is

effectively the combination of Doppler, void and moderator temperature reactivity coefficients.

*[The core is capable of being made subcritical with margin in the most reactive condition throughout an operating cycle with the most reactive control rod, or rod pair, in the full-out position and all other rods fully inserted.]\** This parameter is dependent upon the core loading and is calculated for each plant cycle prior to plant operation of that cycle.

#### 4B.3 CRITICAL POWER CORRELATION

*[The currently approved critical power correlations will be confirmed or a new correlation is established when there is a change in wetted parameters of the flow geometry; this specifically includes fuel and water rod diameter, channel sizing and spacer design.]\**

*[The coefficients for the critical power correlation of a fuel design are determined based on the criteria documented in Reference 4B-2.]\** The fuel design parameters given in these criteria are those that have the primary effect on determining the need for a new critical power correlation when there is a change in the fuel design.

A new correlation may be established if significant new data exists for a fuel design(s). When significant new data have been taken for a fuel design, a better fit to the data may be achieved by adjusting the coefficients in the critical power correlation. The resulting new critical power correlation would be a more accurate representation of actual plant operation. These coefficients are documented in the fuel design information report.

*[The criteria for establishing the new correlation are as follows:*

- *The new correlation shall be based on full-scale prototypical test assemblies.*
- *Tests shall be performed on assemblies with typical rod-to-rod peaking factors.*
- *The functional form of the currently approved correlations shall be maintained.*
- *Correlation fit to data shall be best fit.*
- *One or more additional assemblies must be tested to verify correlation accuracy (i.e., test data not used to determine the new correlation coefficients).*
- *Coefficients in the correlation shall be determined as described in Reference 4B-3 or Reference 4B-4.*
- *The uncertainty of the resulting correlation shall be determined by:*

$$\sigma = \sqrt{\frac{1}{N-1} \sum_{i=1}^N (\mu - \text{ECPR}_i)^2}$$



*Where:*

$\sigma$  = *Standard deviation*

$\mu$  = *Mean*

$N$  = *Total number of data in both the data set used to determine the coefficients and the set used for verification.*

$ECPR$  = *Calculated bundle critical power divided by experimentally determined bundle critical power.]\**

The criteria for establishing a new correlation are those that were used in establishing the correlations approved by the NRC. The basis of the correlation is a best fit of data taken of prototypical test assemblies with typical rod-to-rod peaking factors. *[To ensure that no safety concern exists, the NRC prior to use shall approve the functional form of the current correlation's form. The correlation coefficients and uncertainties are determined in the same manner as approved by the NRC for the current correlations.]\**

#### **4B.4 COL INFORMATION**

None.

#### **4B.5 REFERENCES**

- 4B-1 "GE14 for ESBWR Fuel Rod Thermal-Mechanical Design Report," NEDC-33242P, January 2006
- 4B-2 Global Nuclear Fuel, "General Electric Standard Application for Reactor Fuel (GESTAR II)" NEDE-24011-P-A-15, Class III (proprietary), June 2000, and NEDO-24011-A-15, Class I (non-proprietary), September 2005.
- 4B-3 General Electric Company, "General Electric BWR Thermal Analysis Basis (GETAB): Data Correlation and Design Application," NEDE-10958-PA, Class III (proprietary), and NEDO-10958-A, Class I (non-proprietary), January 1977.
- 4B-4 GE Nuclear Energy Letter, from J. S. Charnley (GE) to C. O. Thomas (NRC), "Amendment 15 to General Electric Licensing Topical Report NEDO-24011-A," January 25, 1986.

NRC RAI 4.2-6

*DCD Tier 2, Appendix 4B.2 states, "For local AOOs such as rod withdrawal error, a small amount of calculated fuel pellet centerline melting may occur, but is limited by the [[ ]]."* The staff has concerns with the ability to accurately model fuel volumetric expansion as fuel enthalpy approached incipient melt temperatures, and the ability to accurately model the evolved fuel pellets in future operation.

*(a) Demonstrate that the fuel thermal expansion/swelling model is capable of accurately predicting volumetric expansion during rapid power changes and at temperatures (1) approaching  $T_{melt}$  and (2) exceeding  $T_{melt}$ . Include a discussion of the model's ability to predict fission-product induced swelling. Provide supporting empirical database, especially test results on irradiated fuel rods.*

*(b) Demonstrate that all of the fuel performance models (e.g. conductivity, expansion, relocation, FGR, grain growth, etc.) remain valid and within their original accuracy for simulating evolved fuel (having undergone partial melt) during future operation including AOOs. Provide supporting empirical database, especially test results on irradiated fuel rods.*

GE Response

10 CFR 50 Appendix A provides an explicit definition of an AOO. 10 CFR 50 Appendix A states "Anticipated operational occurrences mean those conditions of normal operation which are expected to occur one or more times during the life of the nuclear power unit and include but are not limited to loss of power to all recirculation pumps, tripping of the turbine generator set, isolation of the main condenser, and loss of all offsite power." The ESBWR design life is 60 years, and thus, any abnormal event with a probability  $\geq 1/60$  per year must be classified as an AOO, and conversely, any abnormal event with a probability  $< 1/60$  per year should not be classified as an AOO. However, Subsection 15.0.1.2 conservatively defines an AOO "any abnormal event that has an event probability of  $\geq 1/100$  per year."

From Table 15A-3, the most likely RWE has a probability of 1/1000 per year (1 Event in 1,000 yrs). Therefore, the RWE is correctly classified as an infrequent event in Chapter 15, and Tables 15.0-2, 15.0-7 and 15A-3 in Chapter 15 are correct.

DCD Tier 2, Section 4.2 will be modified as noted in the response to RAI 4.2-5. The proposed response will replace the current Section 4B.2 with a reference to the GE14E fuel rod thermal-mechanical design report (Reference 4.2-6.1). Reference 4.2-6.1 will be revised to reflect the discussion above. Specifically, reference to RWE will be replaced by reference to unconstrained control blade maneuvers. Also, the statement that "a small amount of calculated fuel pellet center melting may occur, but is limited by the [[ ]]."

]]." will be removed.

Because of the changes above, the data requested in (a) and (b) is not required and is not included in this response.

Reference

- 4.2-6.1 GE14E Fuel Rod Thermal-Mechanical Design Report, NEDC-33242P, January 2006.

NRC RAI 4.2-7

*DCD Tier 2, Appendix 4B.5 states, "99.9 percent of the rods in the core must be expected to avoid boiling transition for core-wide incidents of moderate frequency..." This criteria differs from GESTAR-II which states, "Ninety-nine point nine percent (99.9 percent) of the rods in the core must be expected to avoid boiling transition."*

- (a) Discuss the basis for this change.*
- (b) Identify AOOs not characterized as "core-wide" and the criteria used to evaluate each.*
- (c) Distinguish between events classified as moderate frequency and those classified as less frequent.*

GE Response

Please see the response to RAI 4.2-6 for discussion of the characterization of events. With the response to RAI 4.2-5 to replace the current Section 4B.2 with a reference to the GE14E fuel rod thermal-mechanical design report (Reference 4.2-7.1) and the response to RAI 4.2-6 to revise Reference 4.2-7.1 to replace reference to RWE by reference to unconstrained control blade maneuvers and to remove the statement that "a small amount of calculated fuel pellet center melting may occur, but is limited by the [[ ]]", there will be no AOO that will not be core-wide. Also, to be consistent with Chapter 15 of the DCD and GESTAR-II, the text in 4B.5 will be revised to read "Ninety-nine point nine percent (99.9%) of the rods in the core must be expected to avoid boiling transition".

Reference

- 4.2-7.1 GE14E Fuel Rod Thermal-Mechanical Design Report, NEDC-33242P, January 2006.

NRC RAI 4.3-3

*In DCD Tier 2, page 4.3-3, reference is made to the lattice code TGBLA06, which has recently been modified to accommodate a minor correction in the programming of analytical formulation in the code. Please submit the modification(s) to TGBLA06. The submittal should include the changes made to the code and validation of the code as it pertains to recent application(s) since the modification of the code, and any natural circulation database, as it pertains to the analysis of the ESBWR steady-state neutronic performance. The contents of the submittal should include before and after calculational results with technical justification(s) in support of the changed results. Also, provide a comparison between the modified TGBLA06 and MCNP results in Section 1.3 of NEDC-33239P.*

GE Response

The TGBLA modification (identified as T6E5) referred to in RAI 4.3-3 is associated with the evaluation of the 1.058 ev. resonance peak under high void conditions (>70% void fractions). The current revision of TGBLA06A is identified as T6E4 for purposes of this discussion. The desire to extend the accepted application range of the TGBLA system to this high void condition (>90%) for study purposes necessitated an improvement in the treatment of the Pu-240 1.058 ev resonance. [[

]] This change will be a function of lattice design, lattice exposure, void history, and instantaneous state of the lattice.

The modification to the Pu-240 1.058 ev resonance evaluation has a small effect on the lattice reactivity and can be best seen by reviewing the Pu-240 concentration prediction. [[

]]

[[

]]

The general impact of the revised TGBLA06 (T6E5) can be seen by reviewing the lattice hot uncontrolled reactivity as a function of exposure and void for the standard design

conditions of 0, 40, and 70% void fraction, the impact of the code modification in the evaluation of lattice parameters at 90% voids from both TGBLA06A computed conditions and the 0, 40, 70 void fraction fitted data evaluations, and the overall impact on an operating cycle of the ESBWR.

Figures 4.3-3-3 and 4.3-3-4 demonstrate the impact of the modified code (T6E5) on the vanished zones in the two (2) proposed ESBWR bundles. [[

]]

Figures 4.3-3-5 and 4.3-3-6 demonstrate the impact on the extrapolation of the hot reactivity to the 90% void condition performed with the modified (T6E5) and unmodified (T6E4) TGBLA06A for the two vanished lattices in the proposed ESBWR design. The reactivity data from the 0, 40, and 70% void depletion state points is fitted as a function of lattice average moderator density and extrapolated to a 90% void condition with a quadratic fit and compared with a TGBLA06A calculated 90% void fraction case. From this, it can be seen that the impact on the fit evaluations at the 90% void history point agrees very well with the computed 90% void history analysis.

Figures 4.3-3-7 and 4.3-3-8 demonstrate impact on the cold reactivity evaluations performed with the modified (T6E5) and unmodified (T6E4) TGBLA06A for the two vanished lattices in the proposed ESBWR design. Here, the impact of the code modification on the evaluation of the cold uncontrolled lattice reactivity for a void history of 90% is evaluated. Again the extrapolation of the fitted data to the computed 90% void history point agrees well.

Figures 4.3-5 through 4.3-8 indicate that the Pu-240 modification has a minor impact on the extrapolation of the 0, 40, 70% lattice reactivity to the 90% void condition and that all three methods (1. extrapolation of T6E4 data, 2. extrapolation of T6E5 data, and 3. the T6E5 computed results) of generating the 90% void history data can be considered identical.

Figures 4.3-3-9, 4.3-3-10, and 4.3-3-11 demonstrate the performance impact of the proposed ESBWR cycle resulting from the code modifications contained in T6E5. [[

]]

This level of perturbation on the core parameters presented in Figure 4.3-3-9, 4.3-3-10, and 4.3-3-11 is considered below the level of significance and the results are considered to be virtually identical.

As a result of the small observed changes in the lattice parameters, it is concluded that the comparisons between TGBLA06 and MCNP found in Section 1.3 of NEDC-33239P continue to be valid. The modified version of TGBLA06 is in the process of internal reviews and will be implemented as soon as all reviews are completed.

No DCD change will be made in response to this RAI.

Figure 4.3-3-1: Pu-240 Concentration for Lattice 81805

[[

]]

Figure 4.3-3-2: Pu-240 Concentration for Lattice 81905

[[

]]

Figure 4.3-3-3: Depletion Evaluation for Hot Uncontrolled Reactivity for Lattice  
81805

[[

]]

[[ Figure 4.3-3-4: Depletion Evaluation for Hot Uncontrolled Reactivity for Lattice  
81805

]]



Figure 4.3-3-5: Fit Evaluation for 90% Void Hot Uncontrolled Reactivity for Lattice  
81905

[[

]]

Figure 4.3-3-6: Fit Evaluation for 90% Void Hot Uncontrolled Reactivity for Lattice  
81905

[[

]]

Figure 4.3-3-7: Fit Evaluation for 90% Void History Cold Uncontrolled Reactivity  
for Lattice 81805

[[

]]

Figure 4.3-3-8: Fit Evaluation for 90% Void History Cold Uncontrolled Reactivity  
for Lattice 81905

[[

]]

Figure 4.3-3-9: Core Reactivity Impact from TGBLA modification

[[

]]

Figure 4.3-3-10: Core Linear Heat Generation Impact from TGBLA modification

[[

]]

Figure 4.3-3-11: Core Critical Power Ratio Impact from TGBLA modification

[[

]]

*Discuss any recent changes made to PANACEA since the staff's last approval. Provide similar information to that requested in RAI 4.3-3. It is presumed that this version of the code is the NRC-approved version of record.*

PANAC11A was reviewed and approved by Letter from Stuart A. Richards to Glen A. Watford, "Amendment 26 to GE Licensing Topical Report NEDE-24011-P-A, GESTAR II - Implementing Improved GE Steady- State Methods (TAC No. MA6481)," November 10, 1999.

The history of the changes in PANAC11A is described below:

PANAC11A	<b>Conversion or Error Correction Details</b>
PANAC11A	<b>Original version, Level 2 ECP on June 9, 1997</b>
PANAC11AE2	<b>First error correction, August 20, 1997 [[</b>
	<b>]]</b>
PANAC11AE3	<b>Second error correction, November 18, 1998 [[</b>
	<b>]]</b>

PANAC11AE4	Third error correction, January 17, 2001 [[
------------	---

[illegible]

PANAC11AE6	Fifth error correction, August 10, 2005. [[
PANAC11AE7	Sixth error correction, September 23, 2005. [[



PANAC11AE8	Seventh error correction, April 20, 2006 [[
------------	---

--	--

NRC RAI 4.4-2

*DCD Tier 2, Section 4.4.1.2 refers to "empirical correlations based on the characteristic dimensions of the fuel bundle and hydraulic properties of the two-phase flow in the fuel bundle" with regards to the void fraction distribution bases. Provide the test data used to develop the empirical correlations and address its applicability to ESBWR operating range. Is this the same void fraction qualification database referred to in Section 4.4.3.2 of DCD Tier 2?*

GE Response

The empirical correlations used for the calculation of the void fraction are the GE void fraction correlation that is used in the 3D core simulator and steady state thermal hydraulic calculations and the correlations for the interfacial shear that is used in TRACG.

The GE void fraction correlation is based on the drift flux model [Reference 4.2-2.2]. The void correlation is correlated as a function of Reynolds number, quality and fluid properties. Since the Reynolds number is a function of mass flux, hydraulic diameter and fluid properties, and the fluid properties are a function of pressure, the void correlation can also be correlated as a function of hydraulic diameter, mass flux, quality and pressure. The parameter ranges for the void fraction data used to develop the void fraction correlation are given in Table 4.2-2-1. It is seen from this table that the parameter ranges cover all GE fuel products and operating ranges.

The GE void fraction correlation is described in detail in the approved Reference 4.2-2.3. The qualification documented in the approved Reference 4.4-2.4, where the void correlation was compared to [[ ]] data points from the most representative full-scale bundles, yielded a standard deviation of [[ ]] in the void fraction, while the qualification against the wider set of [[ ]] data points as documented in References 4.2-2.1, 4.2-2.5 and the approved Reference 4.2-2.6 yielded a standard deviation or [[ ]] in the void fraction (See Table 4.2-2-2).

Table 4.2-2-1. Void Fraction Correlation Database.

Data Source	Geometry	Hydraulic Diameter (m)	Pressure (MPa)	Mass Flux (kg/m <sup>2</sup> -sec)	Inlet subcooling (K)	Exit quality (Max.)	Max void fraction
Simple Geometry	Tube or Annulus	[[					
CISE							
ASEA-513							
GE							
ASEA-713							
ASEA-813							]]

Table 4.2-2-2 Comparison Between Void Correlation and Database  
(Taken from References 4.2-2.5 and 4.2-2.6)

Data Source	Data Points (N)	Average Error $\overline{\Delta\alpha} = \overline{\alpha_m - \alpha_c}$	Standard Deviation $\sigma_{\Delta\alpha}$
CISE GE ASEA-713	[[		
Subtotal			
ASEA-813 ASEA-513			
TOTAL			]]

TRACG uses a two-fluid model where the void fraction is calculated from a balance between interfacial shear and buoyancy. The TRACG correlations for the interfacial shear are derived from an equivalence between drift flux parameters and interfacial shear and has been qualified against data wide range of data including data used for the GE void correlation. The TRACG models for the interfacial shear are described in detail in References 4.2-2.7 and 4.2-2.8, and the application range is summarized in Table 4.2-2-3.

Table 4.2-2-3. TRACG Interfacial Shear Model Application Range

Parameter	Unit	Range
Hydraulic Diameter	m	[[
Pressure	MPa	
Mass Flux	kg/m <sup>2</sup> -sec	
Inlet subcooling	K	
Void fraction		
Data Type		]]

The TRACG qualification is documented in Reference 4.2-2.9. Additional qualification was performed for TRACG in support of the DSS-CD stability solution [Reference 4.2-2.12] and supports the extension of the void fraction range to [[ ]]. The bias and standard deviation for the void fraction prediction have been quantified in References 4.2-2.10 and 4.2-2.11, which approves TRACG including the void fraction model for applications to operating BWRs and ESBWR. For core void fraction prediction the bias and standard deviation in the TRACG void fraction model is reported reference 4.2-2.10 and given in Table 4.2-2-4.

Table 4.2-2-4. TRACG Reactor Core Void Fraction Prediction

	Bias	Standard Deviation
Subcooled Boiling	[[	
Fully Developed Nucleate Boiling and Forced Convection Vaporization		]]

The data used develop the void fraction models are documented in References 4.2-2.1, 4.2-2.8 and 4.2.2.9

The data range and application range for the void fraction models exceeds the expected ESBWR operating range.

The qualification database references in DCD Section 4.4.3.2 is described in References 4.2-2.1 and 4.2-2.9.

#### References

- 4.2-2.1 J. A. Findlay and G. E. Dix, "BWR Void Fraction Correlation and Data, NEDE-21565", January 1977. General Electric Proprietary Information.
- 4.2-2.2 N. Zuber and J. A. Findlay, "Average Volumetric Concentration in Two-Phase Flow Systems", ASME J. Heat Transfer, November 1965.
- 4.2-2.3 "TASC-03A, A Computer Program for Transient Analysis of a Single Channel", NEDC-32084P-A, Revision 2, July 2002.
- 4.2-2.4 Letter, J. S. Charnley (GE) to H. N. Berkow (NRC), "Revised Supplementary Information Regarding Amendment 11 to GE Licensing Topical Report NEDE-24011-P-A", MFN-003-086, January 16, 1986.
- 4.2-2.5 Letter, G. Stramback (GE) to NRC, "Completion of Responses to MELLLA Plus AOO RAIs (TAC No. MB6157)", MFN 04-026, March 4, 2004.
- 4.2-2.6 Methodology and Uncertainties for Safety Limit MCPR Evaluations, NEDC-32601P-A, August 1999.
- 4.2-2.7 J. G. M. Andersen et. al., "TRACG Model Description", NEDE-32176P, Revision 2, December 1999.
- 4.2-2.8 J. G. M. Andersen et. al., "TRACG Model Description", NEDE-32176P, Revision 3, April 2006.
- 4.2-2.9 J. G. M. Andersen et. al., "TRACG Qualification", NEDE-32177P, Revision 2 January 2000.
- 4.2-2.10 TRACG Application for Anticipated Operational Occurrences (AOO) transient Analyses, NEDE-32906P-A, Revision 1, April 2003.
- 4.2-2.11 "TRACG Application for ESBWR", NEDE-33083P-A, March 2005.
- 4.2-2.12 Letter, G. Stramback (GE) to Document Control Desk (NRC), "Responses to DSS-CD TRACG LTR RAIs", MFN 05-133, November 11, 2005.

## **Proposed Changes to ESBWR DCD Tier 2 Chapter 4.4**

### Section 4.4.1.2 Void Fraction Distribution Bases

No changes

### Section 4.4.2.2 Void Fraction Distribution Methods

Replace Section 4.2.2.2 with:

The empirical correlations used for the calculation of the void fraction are the GE void fraction correlation that is used in the 3D core simulator and steady state thermal hydraulic calculations and the correlations for the interfacial shear that is used in TRACG. The GE void fraction model is described in Reference 4.4-15, and details on the qualification are contained in Attachment A to Reference 4.4-13. The TRACG void fraction model is described in Reference 4.4-10 and details on the qualification are contained in Reference 4.4-11.

### Section 4.4.3.2 Void Fraction Distribution Evaluations

Add the References 4.4-11 and 4.4-15 to the sentence:

The void fraction qualification database (*References 4.4-11 and 4.4-15*) contains void fractions in excess of 0.92 and covers the void fraction range expected for normal steady-state operation as well as AOOs.

### Section 4.4-8 References

Replace Reference 4.4-10 with:

- 4.4-10. GE Nuclear Energy, "Licensing Topical Report TRACG Model Description", NEDE-32176P, Revision 3, Class III (proprietary), April 2006.

Add the reference:

- 4.4-15. "TASC-03A, A Computer Program for Transient Analysis of a Single Channel", NEDC-32084P-A, Revision 2, Class III (proprietary), July 2002.

NRC RAI 4.4-5

*DCD Tier 2, Section 4.4.2.1.1 refers to topical report NEDO-10958-A for discussion. Address conditions and limitations applicable to its use for the ESBWR design.*

GE Response

DCD Tier 2, Section 4.4.2.1.1 references NEDO-10958-A, "General Electric BWR Thermal Analysis Basis: Data Correlation and Design Application" which describes the original form of the GEXL critical power correlation and its original development including the experimental qualification and the statistical combination of uncertainties in the formulation of operating limits to assure that 99.9% of fuel rods will not experience Boiling Transition under normal operating conditions and transients. The current NRC approved form of the GEXL correlation (designated GEXL+) was submitted in "Amendment 15 to General Electric Licensing Topical Report NEDE 24011-P-A, January 25, 1986" (GESTAR II) and the approval is contained in Letter, A.C. Thadani (USNRC) to J.S. Charnley (GE), "Acceptance for Referencing of Amendment 15 to General Electric Licensing Topical Report NEDE-24011-P-A, "General Electric Standard Application for Reactor Fuel," Dated March 14, 1988. It is noted that each GE fuel bundle design has a specific set of correlation coefficients based on full scale data. The (GEXL+) critical power correlation developed for GE14 is named GEXL14.

The subject reference (NEDO-10958-A) simply serves as the most complete description of the GETAB methodology. In the context of DCD Tier 2, Section 4.4.2.1.1, this reference serves to describe the method by which the bundle critical power performance is predicted (i.e. the GEXL critical power correlation). As such, it does not have limitations or conditions in application of the GEXL critical power correlation to GE14E for ESBWR; however, it does not demonstrate that GEXL14 (the GE14 specific GEXL correlation) is applicable to GE14E in ESBWR. Applicability of GEXL14 to GE14E operating in an ESBWR is addressed in DCD Tier 2, Reference 4.4-12 (NEDC-33237P issued in March 2006). The initial issue of NEDC-33237P addresses geometric differences between GE14E and the GE14 test assembly (i.e. heated length, spacer locations and part length rod length). The range of fluid conditions over which GEXL must be applied will be addressed in the next revision to this report; however, it is noted here that the range of fluid conditions experienced for ESBWR during normal operation and transients is smaller than that associated with forced circulation BWRs and the existing GEXL14 application range is adequate.

***The ESBWR DCD will be revised as follows:***

**4.4.2.1.1 Bundle Critical Power Performance Method**

The bundle critical power performance methodology is described in References 4.4-8 and 4.4-15. These references describe the form of the GEXL correlation and the experimental qualification that demonstrates the GEXL correlation adequately predicts the bundle critical power over a wide range of fluid parameters, axial power shapes and heated lengths. Each fuel bundle design has a specific set of correlation coefficients

developed from full-scale test data. The specific GEXL correlation applied in the analysis of GE14E for ESBWR is designated GEXL14. The applicability of GEXL14 to GE14E is addressed in Reference 4.4-12.

Revised Reference 4.4-12

- 4.4-12 GE Nuclear Energy, "GE14 for ESBWR Critical Power Correlation, Uncertainty, and OLMCPR Development", NEDC-33237 P Revision 1, Class III (proprietary), scheduled October 2006.

Additional reference:

- 4.4-15 Letter, J.S. Charnley (GE) to C. O. Thomas (NRC), Amendment 15 to General Electric Licensing Topical Report NEDE-24011-P-A, January 25, 1986.



NRC RAI 4.4-6

*The friction pressure drop correlation provided in Section 4.4.2.3.1 of DCD Tier 2, is the same as that used for forced flow in conventional BWRs. Since the ESBWR is a natural circulation reactor with differences in fuel length, spacer separation distance, and partial length rod height, why are there no differences in the friction pressure drop correlation, particularly the two-phase multiplier, which is based on data for conventional BWR fuel bundles?*

GE Response

In the hydraulic models employed in GE/GNF methods, the total bundle pressure drop is defined as the sum of four components: friction, elevation, acceleration, and local losses. In these models, the bundle is also divided into control volumes over which the four components of total pressure drop are evaluated separately, thus allowing to capture the effects on pressure drop of axially variable geometry parameters such as flow area, hydraulic diameter, wetted/heated perimeters, heat flux, and spacer elevations. Furthermore, the single-phase friction factor and two-phase friction multiplier of the correlation provided in Section 4.4.2.3.1 of DCD Tier 2 were validated by extensive comparisons to rod bundle pressure drop data. It should also be noted that the experimental data for current BWR fuel assemblies include the range of mass flux in which the ESBWR fuel assemblies are expected to operate. In particular, the mass flux range for the GE14 pressure drop data, given in Section 2.2 of NEDC-33238P, envelopes the expected range of mass flux conditions for the ESBWR fuel assemblies. It is therefore concluded that the friction pressure drop correlation provided in Section 4.4.2.3.1 of DCD Tier 2 is applicable to the simulation of two-phase flows in ESBWR fuel assemblies.

No DCD change will be made in response to this RAI.

NRC RAI 4.4-15

*The local pressure drop correlation discussed in Section 4.4.2.3.2 of DCD Tier 2, is the same as that used for forced flow in conventional BWRs. (a) What empirical constants were used (and from what source) to fit the results to ESBWR fuel design? (b) How is the single-phase data correlated to two-phase for the fuel assembly components?*

GE Response

The GE core thermal hydraulics methodology expresses the fuel assembly pressure drop as the sum of frictional, acceleration, gravity-head, and local loss components of a total pressure drop. The local loss component of the total pressure drop across a region inside the fuel assembly is deduced from the measured total pressure drop by subtracting the frictional and acceleration components. The corresponding local loss coefficient is then determined from the local pressure formula provided in Section 4.4.2.3.2 of DCD Tier 2. The only empirical constant used in determining the local loss coefficient corresponding to local loss pressure drop across a region inside the fuel assembly is [[

]]. There are four regions in a BWR fuel assembly where experiments are performed to measure the total pressure drop, and the pressure drop data from these experiments are used to determine local loss coefficients: upper tie plate, spacers, flow inside water rods, and bundle inlet. NEDC-33238P provides a detailed description of these experiments performed for the GE14 fuel assembly, and the local loss coefficients obtained with the data from these experiments.

The total pressure drop across bundle inlet and water rods are measured for only single-phase flows. The two-phase losses for bundle inlet and water rods are then calculated using the same two-phase local loss multiplier used for spacers and the upper-tie plate region when a two-phase pressure drop calculation is needed, e.g. LOCA simulations using TRACG.

No DCD change will be made in response to this RAI.

NRC RAI 4.4-16

*DCD Tier 2, Section 4.4.2.3.2 states that new test data are obtained whenever there is a significant design change. Discuss the data available for the ESBWR design and how it is used in the evaluation.*

GE Response

There are four regions in a BWR fuel assembly where experiments are performed to measure the total pressure drop, and the pressure drop data from these experiments are used to determine local loss coefficients: upper tie plate, spacers, flow inside water rods, and bundle inlet. NEDC-33238P provides a detailed description of these experiments performed for the GE14 fuel assembly, and the local loss coefficients obtained with the data from these experiments.

The GE14E design utilizes the same hardware currently used in the GE14 fuel assembly, i.e. the same upper-tie plate, spacers, water rods, and the same bundle inlet design. Therefore, its pressure drop characteristics at the upper-tie plate region, spacers, water rods, and the bundle inlet region remains unchanged. [[

]] In the hydraulic

models employed in GE/GNF methods, the total bundle pressure drop is defined as the sum of four components: friction, elevation, acceleration, and local losses. In these models, the bundle is also divided into control volumes over which the four components of total pressure drop are evaluated separately, thus capturing the effects on pressure drop of axially variable geometry parameters such as flow area, hydraulic diameter, wetted/heated perimeters, heat flux, and spacer elevations. [[

]] It is therefore concluded that the differences between

GE14 and GE14E do not warrant new pressure drop testing of any of the four hardware components, i.e. upper-tie plate, spacers, water rods, bundle inlet, as the same components are utilized in both designs.

It should also be noted that the use of different hardware, e.g. different spacers, would constitute sufficient basis to perform a new pressure drop test for the new ESBWR fuel assembly as stated in Section 4.4.2.3.2 of DCD Tier 2.

No DCD change will be made in response to this RAI.

NRC RAI 4.4-17

*What range of test data discussed in Section 4.4.2.4 of DCD Tier 2, has the pressure drop methodology been qualified to?*

GE Response

The ranges of test data, discussed in Section 4.4.2.4 of DCD Tier 2, are described in NEDC-33238P.

No DCD change will be made in response to this RAI.

NRC RAI 4.4-19

*DCD Tier 2, Section 4.4.3.1.2 refers to uncertainties specific to the ESBWR. Describe these uncertainties and also list conventional BWR uncertainties which are included in the ESBWR design evaluation.*

GE Response

Section 5 of NEDC-33237P (DCD Tier 2 Reference 4.4-12) describes the uncertainties specific to the ESBWR and also provides a discussion of those conventional BWR uncertainties that are applicable to, and thus used as a basis for, the ESBWR design. DCD Tier 2, Section 4.4.3.1.2 text will be replaced to reference Section 5 of Reference 4.4-12 (NEDC-33237P) to provide this clarification. In addition, DCD Tier 2 Reference 4.4-12 description will be updated to reflect this reference's issuance.

***Replacement to DCD Tier 2, Section 4.4.3.1.2 text:***

The Fuel Cladding Integrity Safety Limit (FCISL) is defined as 99.9% of the total fueled rods are expected to avoid boiling transition during normal operation and AOOs. Section 6 of Reference 4.4-12 provides a summary of the basis for the representative operating limit MCPR used for the ESBWR to protect the FCISL. Section 5 of Reference 4.4-12 provides the basis for the uncertainties specific to the ESBWR used in this evaluation.

***Update to DCD Tier 2, Reference 4.4-12 description:***

4.4-12 GE Nuclear Energy, "GE14 for ESBWR - Critical Power Correlation, Uncertainty, and OLMCPR Development", NEDC-33237P, Class III (proprietary), March 2006.

DCD Tier 2 Section 4.4 will be revised as described above.

NRC RAI 4.4-24

*Explain why the test data discussed in Section 4.4.2.3.5 of DCD Tier 2, is applicable to the ESBWR natural circulation flow design with GE14E fuel, considering the differences in active fuel length, spacer separation, and part-length rod height from the tested GE14 fuel.*

GE Response

The GE14E design utilizes the same hardware currently used in the GE14 fuel assembly, i.e. the same upper-tie plate, spacers, water rods, and the same bundle inlet design. Therefore, its pressure drop characteristics at the upper-tie plate region, spacers, water rods, and the bundle inlet region remains unchanged. [[

]] In the hydraulic models employed in GE/GNF methods, the total bundle pressure drop is defined as the sum of four components: friction, elevation, acceleration, and local losses. In these models, the bundle is also divided into control volumes over which the four components of total pressure drop are evaluated separately, thus capturing the effects on pressure drop of axially variable geometry parameters such as flow area, hydraulic diameter, wetted/heated perimeters, heat flux, and spacer elevations. [[

]] Since the differences in active fuel length, spacer separation, and part-length rod height between the GE14 and GE14E fuel designs are accounted for in determining the local loss coefficients from the experimental data, these differences do not impede the applicability of the GE14 pressure drop data to the GE14E fuel design.

Furthermore, the experimental data for current BWR fuel assemblies, discussed in Section 4.4.2.3.5 of DCD Tier 2, include the range of mass flux in which the ESBWR fuel assemblies are expected to operate. In particular, the mass flux range for the GE14 pressure drop data, given in Section 2.2 of NEDC-33238P, envelopes the expected range of mass flux conditions for the ESBWR fuel assemblies.

No DCD change will be made in response to this RAI.

NRC RAI 4.4-27

*The first paragraph on page 3-1 of NEDC-33237P discusses the evolution of the GEXL correlation and references an approved topical report for the R-factor determination. This report addresses GE11, GE12, and GE13 fuel. Explain in detail the changes required for the GE14 fuel design and any GE14E fuel design differences that affect the R-factor determination.*

GE Response

Reference 4.4-27.1 describes the R-factor methodology for the GE11, GE12 and GE13 fuel types that existed at the time when the report was written. The main new features in the fuel that prompted the change in the R-factor methodology was the introduction of part length rods (PLR). In addition the bundle array size also changed from 8X8 to 9X9 for GE11 and GE13 and 10X10 for GE12, but that was not a significant element in the improved R-factor methodology. GE14 fuel is a 10X10 bundle like GE12. The only significant differences between GE12 and GE14 are the spacer design, that the number of spacers was increased from [[ ]] to [[ ]] spacers and that the length of the PLRs was reduced from [[ ]] (heated length) to [[ ]]. Similar differences existed between the GE11 and GE13 designs. No new features affecting the R-factor methodology were introduced with the GE14 fuel design. Had we been able to better predict the future, a more appropriate title for Reference 4.4-27.1 would have been "R-Factor Calculation Method for 9X9 and 10X10 Fuel".

The NRC safety evaluation in Reference 4.4-27.1 contains the condition: "However, if new fuel is introduced, GENE must confirm that the revised R-factor method is still valid based on new test data." This was done for the introduction of GE14 fuel and is documented in Reference 4.4-27.2. The applicable paragraphs from Reference 4.4-27.2 are repeated here:

**GNF Response**

*Calculation of GE14 R-factors follows the approved methodology of NEDC-32505P-A Rev. 1. The R-factor calculations consist of three essential components: the weight scheme for combining rod peaking factors, the additive constants for adjusting individual position performance and the behavior for partially controlled conditions. The weighting scheme of GE14 is identical to that of GE12 because the two bundles are identical in the lattice geometry. The location of the part length rods and the water rods are identical. The main difference is that the length of the part length rods and the spacer locations are slightly different. The additive constants are derived from the test data along with the GEXL coefficients. For partially controlled conditions, the bundle R-factors are calculated based on the prescribed axial power shapes that correspond to the specific GEXL correlation. For GE14, analysis was done to confirm that the partial controlled bundle performances are reasonable using the same process as defined in the approved methodology in NEDC-32505P-A Rev. 1 and the recommendations in the SER.*

Based on the above responses to the conditions of the SER, it is concluded that the GNF 10x10 fuel designs (GE12 and GE14) satisfy the conditions of the SERs.

No changes were introduced to the R-Factor method for GE14E and the above response applies equally well to GE14E.

**References**

- 4.4-27.1 R-factor Calculation method for GE11, GE12 and GE13 Fuel, NEDC-32505P-A, Revision 1, July 1999.
- 4.4-27.2 Letter, G. A. Watford (GNF) to R. Pulsifer (NRC), "Confirmation of 10X10 Fuel design Applicability to Improved SMMCPR, Power Distribution and R-Factor methodologies", FLN-2001-016, September 24, 2001.



NRC RAI 4.4-31

*On page 4-9 of NEDC-33237P, the Mean ECPR value provided [[  
Explain why this is [[ ]] for use in GE14E Operating Limit calculations.*

GE Response

To begin with, recall that the definition of ECPR is:

[[

]]

So, any experimental critical power data-point can have an ECPR. Also, an ECPR greater than 1.0 indicates GEXL over-predicts the critical power and, conversely, an ECPR less than 1.0 indicates GEXL under-predicts the critical power (usually considered conservative). The mean ECPR for a GEXL correlation is simply the arithmetic mean of all individual ECPRs and is included in the methodology that establishes the OLMCPR.

[[

]]

It should be noted that in calculating the OLMCPR, the numerical value will correspond to ~0.1% of rods in BT; however, this is conservative because the conservative GEXL14 mean ECPR will result in a higher MCPR (the OLMCPR) corresponding to this during a limiting transient.

A description of the OLMCPR development process is provided in the response to ESBWR DCD RAI 4.4-32 and will be included in the next revision to NEDC-33237P.

NRC RAI 4.4-32

*On page 5-1, Section 5.1 of NEDC-33237P, the determination of the Operating Limit Minimum Critical Power Ratio (OLMCPR) is discussed. Provide additional discussion of the applicability of the GETAB program (Reference 1) to the ESBWR design.*

GE Response

In Section 5.1 of NEDC-33237P the fourth sentence provides the references (i.e., Appendix IV of Reference 1 and Section 4.6.3 of Reference 5) which contain the details of the procedure (implemented via the GETAB program) for determination of the Operating Limit Minimum Critical Power Ratio. For clarification and simplification this fourth sentence will be replaced with "Details of the procedure are documented in Section 5.13." Then the following will be added as Section 5.13 to this document to provide details of the procedure and discussion of the applicability of the procedure to the ESBWR design. This new section is consistent with Section 4.1 of Reference 6 (which is an updated version of Appendix IV of Reference 1) and Section 4.6.3 of Reference 5.

***NEDC-33237P added Section 5.13 text:***

**5.13 ESBWR Operating Limit MCPR Evaluation Methodology**

The ESBWR calculation procedure for the OLMCPR evaluation is summarized in Figure 5-3, which is a flow chart of the procedure's basic steps. This flow chart is the coupling together in a single flow diagram of the procedures documented in Section 4.1 of Reference 6 and Section 4.6.3 of Reference 5. The flow chart structure highlights the applicability of the overall procedure to the ESBWR. The procedure steps in this figure are based on either ESBWR specific LTRs or are mathematical functions. Each procedure step contains a parenthetical "Input", "3D Simulator", "GEXL", or "Math". Reference 14 is a separate LTR that discusses the "Input" and "3D Simulator" processes applicability to the ESBWR design. Sections 3 and 4 discuss the "GEXL" process applicability to the ESBWR design. The "Math" processes are mathematical functions (e.g. arithmetic, statistical, and integration) that are not dependent on the plant design. A general description of the calculation procedure follows.

[[





[[

]]

**Figure 5-3 Calculation Procedure Basic Steps for OLMCPR Evaluations**

NEDC-33237P will be revised as described above.

NRC RAI 4.4-33

*Section 5.1, page 5-2, of NEDC-33237P, refers to Tables 4.1 and 4.2 of Reference 8, an approved topical report for Power Distribution Uncertainties for Safety Limit MCPR Evaluations. Provide a discussion, qualitative and quantitative, and technical justification for the applicability of this reference to the ESBWR design. Also discuss the applicability of Reference 6 to the ESBWR design.*

GE Response

NEDC-33237P Section 5.1 on page 5-2 reference to Tables 4.1 and 4.2 of Reference 8 is only 'for direct comparison' to conventional BWR values and as such these tables are not being stated as being applicable to the ESBWR design. Referring to these tables was believed to be beneficial in the evaluation of the corresponding ESBWR uncertainty values contained in NEDC-33237P Table 5-1.

NEDC-33237P Sections 5.2, 5.3, 5.4, 5.7, 5.8, 5.11, and 5.13 refer to Reference 6. Section 5.13 is being added as part of the response to RAI 4.4-32. Each of these sections discusses what specific aspect of Reference 6 is being used as a basis and why that basis is applicable to the ESBWR design.



NRC RAI 4.4-34

*Section 1.1 of NEDC-33239P discusses the core physics evaluation model. In the ESBWR evaluation, are all fuel bundles modeled separately, or are individual fuel bundles modeled with an adjustment to account for the effect of adjacent fuel bundles?*

GE Response

A brief discussion of the coupling between lattice physics and the nodal simulator is provided in Section 1.4 of NEDC-33239P. All fuel bundles in the core, which are comprised of a stack-up of individual lattices designs, are modeled separately in the core simulator. All unique lattice designs are modeled with the lattice physics code using an infinite lattice (zero current) assumption. Each node in the three-dimensional core simulator is identified by its unique lattice design and its nodal exposure/void operating history.

During the three-dimensional simulation, all nodes are leakage coupled via the diffusion theory described in Section 1.4.1, thereby accounting for the effects of the adjacency of fuel bundles. One should note that the currents are continuous, but the flux is discontinuous. Following convergence of the global flux and eigenvalue, the linear heat generation rate (LHGR) is determined via a pin power reconstruction method which combines both local peaking effects determined via the lattice physics code and local flux gradients between nodes (and bundles). (Section 1.5.6)

NRC RAI 4.4-36

*Section 1.3 of NEDC-33239P mentions [[ ]]. What [[ ]]  
are being referred to? Were TGBLA06 results ever compared directly to  
the [[ ]]?*

GE Response

The benchmark code MCNP was originally qualified using data from the following critical experiments.

GODIVA and JEZEBEL Experiments  
TRX-1 and TRX-2 Experiments  
The Babcock and Wilcox Experiments  
The ORNL Uranium Nitrate Solution Experiments  
The PNL Plutonium Nitrate Solution Experiments  
The Small Core Critical with and without Poison Curtains  
The Small Core Critical with Burnable Absorbers

A total of 22 critical configurations were modeled explicitly in the original MCNP evaluation suite to form the benchmark bias and uncertainty basis for the use in the TGBLA benchmarking process. These 22 critical experiments are identified below. Note that the experiments 11 through 20 are the "Small Core Critical with Burnable Absorbers" experiments referred to above.

Experiment Number	Experiment Description
1	TRX-1
2	TRX-2
3	B&W UO2
4	B&W MO2
5	ORNL-1
6	ORNL-2
7	PNL-1
8	PNL-2
9	Small Core Critical with Poison Curtain
10	Small Core Critical without Poison Curtain
11	BAG5GD4 at room temperature
12	BAG3GD4 at room temperature
13	BAG3GD16 at room temperature
14	BAG5GD4 at 90°C
15	BAG3GD4 at 90°C
16	BAG3GD16 at 90°C
17	BAG5GD4 at 245°C
18	BAG3GD4 at 245°C – Case A
19	BAG3GD4 at 245°C – Case B
20	BAG3GD16 at 245°C
21	GODIVA Fast Critical
22	JEZEBEL Fast Critical

Subsequent to the original qualification, additional critical experiment evaluations have been added as part of the on-going MCNP evaluation process. Again these critical experiments are exactly modeled in 3 dimensions. Currently MCNP at GNF has been compared to more than 190 Light Water Reactor critical experiment evaluations. All of these experiments were low-enriched (5%  $U^{235}$  or less)  $UO_2$  pin lattice in water experiments. A majority (127) of the experiments are taken from the International Criticality Safety Benchmark Evaluation Project (ICSBEP) handbook. Fifty-two (52) of the experiments contained  $UO_2$  rods with Gadolinium burnable absorber ( $Gd_2O_3$ ) while seventy-seven (77) contained other (non-fuel) structural materials such as stainless steel, Boral, borated steel and aluminum commonly found in spent fuel storage racks. All 190 experiments had material and geometric properties similar to BWR fuel lattices (not including fission product inventories) and are used to benchmark and validate the application of MCNP for both spent fuel criticality safety analyses and BWR lattice physics predictions.

[[

]]

[[

]]

NRC RAI 4.4-37

*Section 1.5 of NEDC-33239P, states that all thermal hydraulic variables are assumed to vary linearly between nodes. Discuss any sensitivity studies performed to demonstrate the appropriateness of this assumption.*

GE Response

Continuity of thermal-hydraulic variables must be maintained between nodes, so a linear approximation for determination of boundary and/or mid-point values is reasonable. All core tracking performed to date, a subset of which is provided in NEDC-33239P, assumes this linear variation between nodes with nodes sizes around 6" (roughly cubic). The reliability and excellent performance of the core simulator in predicting axial power profiles, as seen most clearly in the comparison against TIP data, demonstrates that the power shape is not adversely affected. Changing the number of nodes, thereby altering the nodal axial extent, does not significantly alter that agreement. Therefore it is concluded that the linear approximation for thermal hydraulic variables is appropriate.

NRC RAI 4.4-38

*Section 1.5 of NEDC-33239P briefly discusses crud buildup. Provide details of the evaluation of crud buildup, including the assumptions, modeling, and resulting influence on channel flow rates, pressure drop, rod heat transfer, and nodal power distribution.*

GE Response

Section 1.5 of NEDC-33239P states that a determination of characteristic thermal hydraulic channels is made by assessing "combinations of total channel power, axial power shape, inlet orifice design, channel geometry (e.g., number of fuel rods, spacer design, lower and upper tie plate design), and buildup of crud on the fuel rods". The crud discussed here is the thin layer of tenacious crud that typically builds up on the fuel rods throughout the operating life of the fuel bundle. In GE's standard thermal hydraulic evaluation process, the layer of crud is assumed to exist uniformly on all rods and in all bundles. The typical value used is [[ ]], which represents the condition for a fuel rod averaged over its lifetime. This crud layer has the effect of lowering the in-channel flow area somewhat, as compared to the clean, as-built dimensions, and increasing the surface roughness of the fuel rods. Although these values are different than for a clean bundle, the influence of the crud thickness on the channel flow rates and core pressure drop is very small, 0.1-0.2 psi (0.007-0.014 bar). Nonetheless, this effect is accounted for.

The effect of crud on heat transfer is insignificant in the steady-state methodology since the presence of crud does not affect the liquid film and associated boiling heat transfer. Therefore surface temperatures and heat transfer coefficients are not significantly affected.

Since heat transfer is not significantly affected and the effect on flow rate is small but accounted for, the influence of crud on nodal power distribution is also not significant.

NRC RAI 4.4-42

*What are the values used for the friction correlation constants  $a$ ,  $b$ , and  $c$  in Equation 1.5.3 of NEDC-33239P? What is the reference source? What effect does each constant have on coolant flow and boiling height?*

GE Response

The values used for the single phase friction correlation constants  $a$ ,  $b$ , and  $c$  in Equation 1.5.3 of NEDC-33239P are [[ ]], respectively, for Reynolds numbers above 1084 (a typical Reynolds number is on the order of  $2 \times 10^5$  for in-channel flows). These coefficients are given by Equation 6.2-2 in the TRACG Model Description document, NEDE-32176P, Rev. 2. NEDC-33239P refers to the approved application document for TRACG application to ESBWR (NEDE-33038P-A), which incorporates this model description document by reference. An updated version of the TRACG Model Description, NEDE-32176P, Rev. 3, was provided to NRC in April 2006 for review. The single-phase friction correlation is unchanged from the earlier revisions. The friction correlation model is common to core thermal hydraulic modeling in the steady-state core simulator, PANAC11, and TRACG.

The form of the single-phase friction factor is well established. The single-phase friction factor referred to is calculated from a fit to the Moody curves [J. Waggener, *Friction Factors for Pressure Drop Calculations*, Nucleonics, 19 (11), November 1961]. For laminar flow, the friction factor results from the exact solution for fully developed flow in circular pipes. For turbulent flow in smooth pipes, Blasius and McAdams proposed correlations that approximate the Prandtl - Von Karman - Nikuradse line over a wide range of Reynolds numbers. In 1939, Colebrook extended the expression for turbulent flow in a smooth pipe to include roughness of the pipe wall in the so-called transition region between smooth pipe flow and flow for which  $f$  is constant. Moody, in 1941, presented the Colebrook function in the well-known Moody diagram. The subject equation 1.5.3 of NEDC-33239P is an approximation proposed by Moody in 1947 to Colebrook's function, which includes the effect of roughness.

The influence of the correlation coefficients on the coolant flow is very small. The largest influence obviously comes from the coefficient  $a$ , which is linearly related to the friction factor,  $f$ . For instance, a 10% change results in a pressure drop change on the order of 0.1 psi (0.007 bar). The resulting influence on core flow of such a flow resistance change is only on the order of 0.4%. The other two coefficients have a lesser influence on core flow since the friction factor varies only as the cube root of terms containing  $b$  and  $c$ . The effect of friction on heat transfer is insignificant and the core flow is also insignificantly affected. Therefore, there is no significant effect on boiling height.

NRC RAI 4.4-43

*What is the assumed value of the surface roughness,  $\epsilon$ , in Equation 1.5.3 of NEDC-33239P? Also, what is the source of the friction factor correlation constants in Equation 1.5.3? If surfaces are not smooth, what is the impact on boiling height?*

GE Response

The value of the surface roughness used is [[ ]], which covers the condition for a fuel rod averaged over its lifetime. This crud layer has the effect of increasing the friction of the fuel rods as compared to the clean, as-built dimensions. Although these values are different than for a clean bundle, the influence of the crud roughness on the channel flow rates and core pressure drop is not large, 0.3-0.4 psi (0.021-0.028 bar). The effect of the crud layer thickness was addressed in the response to RAI 4.4-38. Nonetheless, it is considered in the process that the surfaces are not smooth. Therefore a roughness that matches historically observed core plate pressure drops is used so that this effect is properly accounted for. The ESBWR for component surface roughness, including the effects of crud, is expected to be the same as for the rest of the BWR fleet.

The effect of surface roughness on heat transfer is insignificant in the steady-state methodology since the presence of crud does not affect the liquid film and associated boiling heat transfer. Therefore surface temperatures and heat transfer coefficients are not significantly affected, which in turn results in no significant change in the boiling height.

NRC RAI 4.4-44

*Section 1.6.3 of NEDC-33239P, provides the procedure for performing gamma scanning and highlighting the performance of PANAC11 against TIP data. Are the results of PANAC11 adjusted results?*

GE Response

The comparisons of PANAC11 TIP response predictions to TIP data in Section 1.6.3 of NEDC-33239P are comparisons between best estimate predictions (unadapted) and the instrumentation. These are unadjusted results.

The gamma scans comparisons must be applied consistently with the context of the SLMCPR power distribution uncertainties. Since the SLMCPR methodology details the adaptive technology, these gamma scan comparisons are done between measured data and predictions that have been corrected for the axial shape predicted by the TIPs. The effect of this adaption on the gamma scan comparison is rather small since there are only a few TIP calibration opportunities near the end of cycle, and the signature of interest is the  $^{140}\text{Ba}/^{140}\text{La}$  gamma ray that is proportional to the integrated power distribution over the last ~60 days of steady operation.



NRC RAI 4.4-45

*Section 1.6 of NEDC-33239P, Figure 1-26, provides insight into the eigenvalue trend with burnup. Explain the [[ ]]. Also, explain the [[ ]].*

GE Response

Figure 1-26 of NEDC-33239P provides the hot operating eigenvalues for a variety of BWRs, as predicted by PANAC11, the GE 3D core simulator, for actual reactor operating statepoints. The downward trend in eigenvalue with cycle exposure is very typical for plants with longer operating cycles (18 to 24 month refueling intervals) and mid-sized to large batch fractions of fresh fuel (25% batch fraction and greater). While this trend is characteristic of the core simulator method, it is difficult to clearly establish the reasons for the systematic change in eigenvalue with exposure. Gadolinia content, U-235 enrichment, control blade depletion, Pu fissile isotopic buildup and the various fission product inventories all change with cycle exposure. The simulator's level of accuracy is to a degree correlated to the magnitude of nodal isotopic contents and the reactivity worth of these components and so resulting eigenvalues reflect those trends.

The eigenvalue trends are relatively stable in regards to the amount of eigenvalue change with cycle exposure, are relatively consistent cycle-by-cycle for a given plant, and are consistent over a wide range of operating plants. Figure 1-26 illustrates that this eigenvalue trend is relatively stable with a [[ ]]

[[ ]] is relatively consistent between the various operating plant/cycles. The [[ ]] in eigenvalue for some of the high energy cycles depicted in Figure 1-26 is typically the result of end-of-cycle extensions, such as increased core flow operation or power coastdown. Such operational changes result in a noticeable shift in core axial power shape and can have an effect on predicted eigenvalues.

The eigenvalue trend in PANAC11 has substantially reduced this drop relative to previous versions, reducing [[ ]]

[[ ]], even as batch fractions, discharge exposure and bundle enrichments have continued to increase. This type of consistency between plants and operating cycles has allowed GE and the utilities to make reasonable predictions of expected future performance in regards to reactivity, cycle energy, fuel performance and reactor thermal margins.

NRC RAI 4.4-46

*Section 1.6.5 of NEDC-33239P, Cold Critical Measurements, states that the negative trend alluded to in Figures 1-26 and 1-27 is accounted for in the design process. Provide additional supportive information to this effect.*

GE Response

Similar to Figure 1-26, Figure 1-27 provides the cold operating eigenvalues for a variety of BWRs, as predicted by PANAC11, for actual reactor cold critical statepoints. Similar to the hot eigenvalue, the downward trend in cold eigenvalue with cycle exposure (particularly for the first half of the operating cycle) is very typical for plants with long operating cycles and mid to large batch fractions of fresh fuel. The same phenomena that were discussed in the response to RAI 4.4-45 also affect the calculation of cold reactivity as a function of cycle exposure.

In establishing an expected cold eigenvalue behavior for an upcoming design cycle, the selection process can be divided into two parts: first, the selection of the beginning of cycle (BOC), and second, the expected trend, or drop, in eigenvalue from this BOC value with cycle exposure. The division of the selection into these two separable components is done for practical reasons. Unlike the hot operating eigenvalue, where information (operating statepoints) is available on a continuous basis throughout the cycle, the cold critical data is consistently available only for the BOC condition. The plant will always perform a BOC critical, both to satisfy the Technical Specification shutdown margin demonstration requirement, and as the initial step in bringing the reactor to power. However, later in a cycle, data are only available if the reactor experiences an unexpected shutdown during the cycle for a length of time which allows xenon to decay, permitting a clean, cold critical.

Based on this, the BOC expected cold eigenvalue can be established, relying heavily on the plant previous cycle BOC information. The selection of the behavior of the cold eigenvalue with cycle exposure is more difficult due to the lack of plant specific data. Because of this, the exposure behavior is normally selected using a generic trend, established by observing the cold eigenvalue drop (relative to BOC) from [[  
]]. For this generic database, the mid-cycle cold critical eigenvalues were compared to the BOC eigenvalue for the same plant/cycle, and the change in eigenvalue relative to BOC as a function of cycle exposure is examined. (As can be observed in Figure 1-27, the cold eigenvalues tend [[  
]].) This database is used to establish a best estimate/slightly conservative trend of cold eigenvalue drop with cycle exposure relative to BOC. By using this generic trend in combination with the plant specific BOC cold eigenvalue, the expected cold eigenvalue as a function of cycle exposure is established.

NRC RAI 4.4-47

*Are the RMS results provided in Table 1-17 using TIP-adjusted PANAC11 predictions?*

GE Response

Table 1-17 provides the summary core-wide statistics of TIP comparisons for the reference plants. The comparisons are between the best-estimate predictions of the instrument response versus the six inch (nodal) average of the measured instrument responses. There is no adaption (or any other adjustment) performed on the prediction. The data indicate that PANAC11 is doing an excellent job of power shape prediction for modern fuel designs and plant operation strategies.

NRC RAI 4.4-48

*Section 1.7 of NEDC-33239P, Reactivity Coefficient Methods, references an NRC-approved lattice physics code. State the code referenced.*

GE Response

All lattice calculations used for the reactivity coefficient analyses, steady state thermal limit analyses, and reactivity analyses were based from the currently approved lattice physics code TGBLA Version 6. Similarly, the currently approved nodal physics simulator PANACEA Version 11 (PANAC11) was used for all 3D simulations. These codes and versions are identical to the methods used in the other BWR operating plants.

NRC RAI 4.4-49

*Section 1.7 of NEDC-33239P states that all the calculations were performed as a function of void fraction and at various standard hot uncontrolled exposure depletion points. Provide specific details, in tabular form, including the void fraction values and explanation of standard hot depletion points. Discuss any sensitivity studies which have been performed to assess the effect of perturbations of pressure and core flow.*

GE Response

The following table provides all of the standard hot uncontrolled Doppler exposure points. For each exposure, lattice calculations for 0% void, 40% void, and 70% void were performed. Figure 3-57 and Figure 3-58 of NEDC-33239P provide an example comparison for a dominant lattice at 40% void for each of the two bundle types. The red boxes within these two figures correspond to the exposures in the below table.

Sensitivity studies have not been performed to assess the effect of perturbations of pressure and core flow.

Exposure GWD/st	Hot Uncontrolled		
	0 Void	40 Void	70 Void
0			
0.2			
1			
3			
5			
7			
8			
9			
10			
11			
12			
13			
14			
15			
17			
20			
30			
40			
50			
65			

NRC RAI 4.4-50

*Section 3.0 of NEDC-33239P, Figures 3-1 through 3-6, indicate a bundle designation [[ ]] in the title.*

- a) It is assumed by the staff that the fuel type used in the analysis of the referenced core (alluded to in section 3.1 of NEDC-33239P), is the GE14E and not the [[ ]]? If so, shouldn't the designation in Figures 3-1 through 3-6 be GE14E? Also, is the "referenced core" the same as an initial core, or an equilibrium core?*
- b) If this is the GE14E, provide a description of the final fuel design used in the analysis.*
- c) The designation in the titles of these same figures also suggest that these computer runs were conducted using PANACEA 10. Is that correct? Please clarify.*

GE Response

Section 3.0 of NEDC-33239P provides descriptions of the enrichment and gadolinia composition of the fuel assemblies used for the DCD core design. Each fuel assembly (there are two) and constituent lattice (a total of 12) has a unique name that differentiates it from other fuel assemblies and fuel lattices. There exists a nomenclature key to the naming convention for GE internal purposes that is subject to change. It should be noted that the moniker "GE14E" has been used as a convenience for communicating with the staff when discussing GE14 as it applies to the ESBWR. It is considered that the fuel assembly used in the DCD is of the GE14 family (as opposed to a GE13 or GNF2 family). Within the name, there exists sufficient information to uniquely determine that the application of the bundle is for ESBWR, most visibly the active fuel height. An associated nomenclature key exists for the lattice names.

The features in question for the names used in the DCD are explained below.

- a) The names of the bundles in the DCD core design are [[ ]] and [[ ]]. The "GE14" prefix places this product in the GE14 family (which GE14E is). The identifying portions in the remainder of the name that associate these bundles with ESBWR are the "N" after the "P10" and the "-120-". This represents the lattice type (N-lattice) and active fuel length, which is 120 inches for ESBWR, respectively. The naming convention does not call for the use of a "GE14E" designator to earmark this bundle for use in ESBWR applications. The "referenced core" is the core design for the DCD, which is an equilibrium core, representative of core design and operation for cycles after the initial cycle.
- b) The fuel designs shown in Figures 3-1 through 3-6 in NEDC-33239P are the final fuel designs used in the DCD core design.
- c) The "P10" does not refer to a PANACEA version number. It refers to the pre-pressurization in atmospheres of the fuel rods. All steady-state core simulations in the DCD are performed using PANAC11.

NRC RAI 4.4-52

*Explain Figures 3-7 through 3-21 in section 3.0 of NEDC-33239P and why there are no figures representing the higher void fraction conditions. How does the linear fit of void fraction data compare to TGBLA at 90% void conditions?*

GE Response

Figure 3-7 through 3-12 and Figures 3-16 through 3-21 in Section 3.0 of NEDC-33239P contain infinite lattice local peaking data for the constituent lattices of the bundles 90018 and 90019, respectively. Note that bundles and lattices are designated both by name and by number, each of which is a unique identifier. These data are the maximum 2-D, infinite lattice pin powers at each exposure step in the depletion for each of the void histories for which TGBLA06 is run. Since the standard process does not involve [[ ]], these values are not present in these figures. These maximum pin power peaking values include the effect of gamma energy deposition on the pin power distribution.

Figure 3-13 is the pin-by-pin distribution of relative power for the dominant lattice in bundle 90018, designated by the lattice number 81802. This again is the 2D, infinite lattice peaking. It is for an in-channel void fraction of 40% and at beginning-of-life.

Figure 3-14 is the fully uncontrolled and fully controlled bundle R-factor as a function of bundle average exposure for bundle 90018.

Figure 3-15 is the distribution within the bundle of the fully uncontrolled pin-wise R-factors at an exposure of 20 GWD/ST. This exposure is chosen because critical power is typically limiting at the end of cycle, and it is usually the first cycle bundles that are limiting at this point in the cycle. Only the maximum of this distribution becomes the bundle R-factor. One can see that the uncontrolled bundle R-factor from Figure 3-14 at this exposure is 0.9621. This value corresponds to the maximum value in Figure 3-15, which occurs at [[ ]].

The comparison of the fit ([[ ]]) of relative pin power is performed on a pin-by-pin basis. The maximum value from the resulting distribution is taken as the maximum lattice pin power value. The comparison of the maximum pin power from the fit compared to the run of TGBLA is given in the figures below for two of the vanished zone lattices (those above the part length rods). These lattices are the enriched lattices that experience the highest in-channel void fraction. These correspond to Figures 3-11 and 3-20 in NEDC-33239P. In summary, the maximum 2D infinite lattice pin power as determined by the fit at 90% in-channel void fraction is different from the run with TGBLA only for high exposures when the reactivity of the lattice is low and even then, the peak pin error is within the nominal pin power distribution error for the code.

No DCD changes will be made in response to this RAI.

Figure 4.4-52-1      Lattice 81805 Maximum Local Peaking vs. Exposure  
[[

]]

Figure 4.4-52-2      Lattice 81905 Maximum Local Peaking vs. Exposure  
[[

]]



NRC RAI 4.4-53

*Figure 3-33 of NEDC-33239P represents the shutdown margin with exposure. Is this for all rods in, or just the shutdown banks? Provide additional discussion of the physics behind the shape of the curve in the figure.*

GE Response

Figure 3-33 represents the exposure dependent 3-D shutdown margin to criticality with all rods in, with the highest worth rod (or rod pair) withdrawn from the core. The highest worth rod is determined by withdrawing multiple rods individually, until the rod with the greatest impact on core wide reactivity is determined.

The shape of the exposure dependent limiting shutdown margin is very similar to the rest of the BWR fleet. A curve that is limiting at BOC, less limiting towards MOC, and begins to fall again towards EOC is typical of the effect on reactivity due to gadolinium burnout and fissile depletion. Had more gad rods been incorporated into the fresh bundle designs additional BOC SDM would result, at the expense of BOC hot excess. Had less gad rods been included in the fresh bundle designs, less BOC SDM would result, with an increase of BOC hot excess. A BOC minimum design shutdown margin of 1.5% is considered to be more than adequate when taking into account methods and operational uncertainties. The SDM towards the end of cycle is primarily influenced by the selection of the gadolinium concentration (weight %). If more concentration were included in the gad rods, more SDM towards EOC would result. Similarly, if less concentration were included in the gad rods, less SDM towards EOC would result.

At BOC the cold axial flux shape is often mid peaked. Consequently, gad rods towards the middle of the bundle are more significant in controlling cold reactivity. As the core burns through the cycle with a hot axial shape towards the bottom of the core, plutonium generation towards the top of the core results (along with a lessened U-235 depletion). This combination produces a cold axial flux peak that is higher and stronger towards the top of the core. Therefore, gad concentration weight percents higher in the bundle are more significant in controlling cold reactivity and shutdown margin towards the middle and end of cycle.

For the cold reactivity condition xenon does not play an important role because the maximum reactivity condition is achieved in a cold, xenon-free condition.

NRC RAI 4.4-54

*In Figures 3-37 through 3-41 of NEDC-33239P, reference is made to comparison with a limit. Clarify what limit is being referred to. On page 3-8 of NEDC-33239P, the MCPR is discussed briefly. The staff requests clarification of figures 3.41 through 3.44, with supporting discussion regarding what rod patterns are being referred to, what exactly is being ratioed, and what parameter is being defined as 1?.*

GE Response

In Figure 3-37, the Maximum Fraction of Linear Power Density (MFLPD) is presented as a function of cycle exposure. Note that the value plotted in Figure 3-37 represents the maximum value for any node in the core at the specified exposure point. The MFLPD parameter, in general terms, is defined as:

$$\text{MFLPD} = \text{LHGR} / \text{LHGR Limit}$$

It should be noted that the thermal mechanical LHGR limit is exposure dependent which necessitates establishing the MFLPD parameter to capture this. A MFLPD that is equal to 1.0 corresponds to a rod in a node that is operating on its LHGR limit and any further increases in LHGR result in entering a Technical Specification LCO condition. Every rod within a node has a MFLPD. The rod with the highest MFLPD in any given node defines the maximum MFLPD and this is then the nodal MFLPD. The node with the highest MFLPD in an assembly can be thought of as the limiting MFLPD for that assembly. The highest MFLPD for any node in the core corresponds to the most limiting node and defines the minimum operating margin (1.0 – MFLPD) in the reactor core. Figures 3-38 through 3-40 depict the distribution of assembly maximum MFLPD values in a quarter core.

The case is similar for the CPRRAT values displayed in Figures 3-41 through 3-44. The CPRRAT has a slightly different definition, however:

$$\text{CPRRAT} = \text{OLMCPR} / (\text{Assembly CPR})$$

The OLMCPR for the ESBWR DCD was assumed to be [[ ]] and has been calculated to be [[ ]] and reported in NEDC-33237P. For the graphs presented in this report, the OLMCPR value of [[ ]] was used as reference.

Every assembly has a CPR and any assembly with a lower CPR than the OLMCPR results in entering a technical specification LCO condition. As such, any assembly with a CPRRAT value of 1.0 corresponds to operating on limits. The assembly with the lowest CPRRAT is then the most limiting assembly in the core. Figure 3-41 corresponds to the limiting CPRRAT throughout the operating cycle (the limit is 1.0). Figures 3-42 through 3-44 depict the distribution of assembly CPRRAT throughout a quarter core at several exposure points through the cycle.

The rod patterns are those depicted in Figure 3-28 at the corresponding cycle exposure points.

This will be clarified in Revision 1 to NEDC-33239P

NRC RAI 4.4-55

*Provide an explanation of Figures 3-55 through 3-60.*

GE Response

Figure 3-55 is comprised of tables of 3D core neutron multiplication at critical control rod patterns developed at 100°C at which boiling can occur. The 3D core simulation (0 voids at various temperatures at several points through the cycle) is then repeated with nuclear libraries generated with an in-channel void fraction of 5%. The 3D neutron multiplication at 0% and 5% voids are the key inputs into the determination of the cold void coefficient. Figure 3-56 is then the cold void coefficient as a function of moderator temperature at several exposure points through the cycle and confirms that the ESBWR maintains negative void coefficients.

Figures 3-57 and 3-58 depict infinite lattice neutron multiplication values as a function lattice exposure at the 2 temperatures established for the determination of the Doppler coefficient. The label HOTUNC corresponds to an average fuel temperature of [[        ]] and HOTUNCD corresponds to an average fuel temperature of [[        ]].

NRC RAI 4.4-56

*In reference to Section 4.4.2.1.2, provide additional quantitative discussion of the transient  $\Delta$ CPR/ICPR and statistical uncertainty associated with the critical power correlations. Also provide values for manufacturing tolerances, parameter measurement, and calculation uncertainties. Discuss any conditions and limitations of the referenced approved Topical Reports which are applicable to the ESBWR design.*

GE Response

DCD Tier 2 reference 4.4-12 (NEDC-33237P) provides additional quantitative discussion of the uncertainties used in the determination of the Operating Limit MCPR for the ESBWR design. NEDC-33237P provides the requested additional information as follows:

1. Section 5.12 of NEDC-33237P provides additional quantitative discussion of the transient  $\Delta$ CPR/ICPR
2. Section 4 of NEDC-33237P provides additional quantitative discussion of the statistical uncertainty associated with the critical power correlation
3. Section 5 of NEDC-33237P provides the basis for manufacturing tolerances, parameter measurement, and calculation uncertainties for the various uncertainties used in the OLMCPR development

DCD Tier 2 Section 4.4.2.1.2 first four sentences will be revised, as shown below, to replace the conventional BWR references 4.4-8 and 4.4-13 with the corresponding ESBWR reference 4.4-12 (NEDC-33237P) and to provide some clarification.

With the removal of the approved conventional BWR references 4.4-8 and 4.4-13 from the DCD Tier 2 Section 4.4.2.1.2, the only remaining referenced LTRs are the AOO sections of Reference 4.4-9 and Reference 4.4-12, which have not been approved. Reference 4.4-9 AOO sections and Reference 4.4-12 in its entirety has been submitted to the NRC as part of the ESBWR Design Certification Application.

***Revision to first four sentences of DCD Tier 2 Section 4.4.2.1.2 text:***

The statistical analysis utilizes a model of the core that simulates the core monitoring system. The model produces a critical power ratio (CPR) map of the core based on steady-state uncertainties defined in Table 5-1 of Reference 4.4-12. This is coupled with the TRACG  $\Delta$ CPR/ICPR results to develop the OLMCPR. Details of the procedure are documented in Section 5.13 of Reference 4.4-12 and Subsection 4.6.3 of Reference 4.4-9.

DCD Tier 2 Section 4.4 will be revised as described above.

NRC RAI 4.8-1

*The GE14E fuel assembly description in Section 2 of NEDE-33240P does not identify any debris filtration components. Provide a description and drawing of any debris filtration components, if applicable. Include a discussion of the effectiveness of the design in trapping debris.*

GE Response

Figure 2-8 of the GE14E Fuel Assembly Mechanical Design Report NEDC-33240P depicts the debris filter lower tie plate. Additional details of the lower tie plate casting are shown in Figure 4.8-1-1. [[

]] The GE14E design uses the same lower tie plate as the GE12/14 DF design.

Figure 4.8-1-1 GE14E Lower Tie Plate Casting Detail (Note dimensions are in inches)  
[[

]]

Figure 4.8-1-2 Lower Tie Plate Flow Path Size

[[

]]

NRC RAI 4.8-2

*The Zircaloy-2 processing described in Section 2.2 of NEDE-33240P includes the sentence: "If more significant process changes are made, the applicability and adequacy of the properties will be confirmed." As indicated in this section, changes in material composition and manufacturing process have the potential to impact the material properties of the finished Zircaloy-2.*

- (a) Describe the manufacturing quality control procedures which will be in place to ensure that future lots of fuel assembly components exhibit the same performance characteristics as provided in NEDE-33240P.*
- (b) Describe the manufacturing change process which will be in place to ensure that future lots of fuel assembly components (manufactured with changes in the fabrication process) exhibit the same performance characteristics as provided in NEDE-33240P.*

GE Response

In accordance with 10CFR50 Appendix B, all GNF fuel product is produced under a comprehensive system of controls as implemented through levels of documented procedures and instructions, instilled through active training programs, and continually evaluated and reinforced by independent Quality Control organization oversight. The rigor enforced through this comprehensive control system ensures that the final GNF fuel product, including the effects of any manufacturing process changes, conforms to all specified requirements.

As suggested by the NRC reviewer, the fuel rod cladding [[  
]] will be used as the example for specific response to this item.

Manufacturing Quality Control Procedures

[[



]]

[[

]]

Manufacturing Change Process

[[

]]

NRC RAI 4.8-3

*Section 3.1 of NEDC-33240P addresses dimensional changes of assembly components. This section does not address part-length fuel rod growth and design margin to accommodate differential growth relative to the spacer positioning water rod. Please address this issue.*

GE Response

There is substantial margin relative to the differential growth between the top of the part-length rod (PLR) and the adjacent spacer elevation. [[

]]

NRC RAI 4.8-4

*Section 3.1 of NEDC-33240P addresses dimensional changes of assembly components. This section does not address differential assembly growth and design margin to ensure channel fastener spring engagement within a control cell. Please address this issue.*

GE Response

There is adequate margin relative to differential bundle growth with respect to channel fastener spring overlap. [[

]]

NRC RAI 4.8-5

*Figures 3-3, 3-6, and 3-9 of NEDE-33240P provide measured irradiation-induced growth data taken from current GE fuel designs.*

*(a) Discuss the applicability of these previous measurements to the GE14E design. Identify the material composition and manufacturing process for each of the data sets.*

*(b) Discuss the linearity of the data.*

GE Response

- a) Fuel rod, fuel bundle and water rod data are for [[  
]] material. Channel data are for [[  
]] materials. These materials and  
processes are the same as those for the GE14E fuel design. [[  
  
]]
- b) The available growth measurements for the GE14E exposures, the margins provided by the GE14E design, and the conservative application of BWR/4-6 data to the ESBWR fuel length make the linear approximation a reasonable basis for assessment. [[

]]

NRC RAI 4.8-6

*Section 3.3.1 of NEDC-33240P states, "These limits are typically applied to unirradiated material conditions because irradiation increases the material strength properties." While it is true that irradiation hardening increases the material yield strength, it may not increase the overall strength of a component such as a spacer. Describe the steps taken (e.g. irradiated material testing) to ensure that the beginning-of-life evaluations are most limiting.*

GE Response

During operation, the strength of Zircaloy structural components increases due to hardening resulting from fast neutron fluence. The only currently identified mechanisms that could reduce the overall strength of fuel assembly components with in-core operation are [[

]] GNF structural evaluations explicitly address the reduction in strength [[ ]], so a reduction in strength of irradiated components relative to the strength at beginning-of-life would be due [[ ]]. As discussed in the combined response to RAIs 4.2-2 and 4.2-4, GNF has performed tests to confirm that [[

]]. This supports the assumption that component strength is most limiting at beginning-of-life.

This has been confirmed by tests on specific components. [[

]]

[[

]] These results show that the fracture resistance of the spacer material and structure remains high enough to avoid failure [[

Figure 4.8-6-1 Hydride Spacer Test Fixture

[[

]]

Figure 4.8-6-2 Typical Force Time History

[[

]]

Figure 4.8-6-3 Force Time History with Crack Development

[[

]]

Figure 4.8-6-4 Hydride Spacer Test Results

[[

]]



NRC RAI 4.8-7

*Section 3.3.3 of NEDC-33240P states, "Testing is performed to assure that the mechanical features of the design do not result in significant vibration and consequent fretting wear."*

- (a) Provide the flow induced vibration (FIV) test results for the GE14E assembly design.*
- (b) Discuss the impact of in-reactor dimensional changes (e.g. fuel rod growth, grid spring relaxation, etc.) on the adequacy of laboratory testing of unirradiated samples.*
- (c) If specific GE14E FIV test results have not been conducted, demonstrate the applicability of previous FIV test results to the GE14E design. Describe any differences in assembly design e.g. part-length rods, grid springs, grid elevations, materials, etc.) which may potentially impact the FIV test results.*

GE Response

- a) FIV testing specifically for GE14E has not been performed to-date. GE will confirm by test the FIV performance of the GE14E design prior to the delivery of the GE14E fuel. As discussed below, the similarity of the GE14 and GE14E designs, tests previously performed for GE14 for BWR/4-6 reactors, and many years of successful in-reactor operation of the GE14 design provide assurance that FIV will not be a significant issue for GE14E.
- b) [[  
  
]]
- c) With respect to potential for fretting caused by FIV, the GE14E design is nearly identical to GE14. [[

]]

NRC RAI 4.8-8

*Section 3.4.1.11 of NEDC-33240P describes the seismic and dynamic loads, including hold down margin, acting on the fuel assembly during normal and accident conditions. Conclusions are qualitative and lack the necessary information for the staff to make a determination. Provide a quantitative assessment of seismic and dynamic loads for the GE14E fuel assembly design including supporting mechanical test data and the resulting fuel design requirements.*

GE Response

The current production GE14 design for BWR/4-6 and ABWR applications has been demonstrated to meet the criteria of the requirements stipulated in NEDE 21175-3-P-A, "BWR Fuel Assembly Evaluation of Combined SSE and LOCA Loadings (Amendment No. 3)", for bounding seismic accelerations of [[

]]

The following evaluations have been performed to assure that the GE14 fuel assembly satisfies the acceptance criteria for the bounding dynamic loads. The acceptance criteria are that the primary stresses are less than 70% of the material ultimate strength, or that a test demonstrating margin for sustaining the applied loads is performed. The evaluations are performed considering only primary loads and using unirradiated material properties.

Fuel rod evaluation

[[

]]

[[

]]

[[

]]

Water rod evaluation

[[

]]

[[

]]

[[

]]

Spacer evaluation

[[

]]

Upper tie plate evaluation

[[

$$S_b = \frac{Mc}{I} = [[ \quad \quad \quad ]]$$

The unirradiated ultimate tensile strength for stainless steel castings at rated operating temperature is 407 MPa. The ratio of allowable stress to predicted stress is

$$\frac{\text{Allowable stress}}{\text{Predicted stress}} = \frac{0.7 \times S_u}{S_{\max}} = [[ \quad \quad ]]$$

Lower tie plate evaluation

[[

]]

[[

]]

Channel evaluation

[[

]]

[[

]]

Using this scale factor, the adjusted loads corresponding to the [[ ]] dynamic load is

[[

]]

[[

]] The ratio of the test load to the predicted load (including the scale factor) is

[[

]]

[[

[[ ]]

[[

]]

Scale Factor = [[ ]]=1.8

[[

]] The ratio of

channel capability to the test load is

$$\frac{\text{Test load}}{\text{Predicted load (scaled)}} = [[ ]]$$

#### Summary of results

Each of the major fuel assembly components has been evaluated to the criteria described above. A summary of the results for each component is given in the following table.

Component	Method of Evaluation	Margin <sup>a</sup>
Fuel rod	Analysis	[[
Water rod	Analysis	
Upper spacer	Test	
Lower spacer	Test	
Upper tie plate	Analysis	
Lower tie plate	Test	
Channel	Test	]]

<sup>a</sup> – The ratio of allowable stress to the predicted stress, or the ratio of the test load to the predicted load.

Figure 4.8-8-1 Fuel Assembly Acceleration Profile

[[

]]

Figure 4.8-8-2 Spacer Seismic Test Fixture

[[

]]



Figure 4.8-8-3 GE14 Upper Tieplate Water Rod Boss Loading and Moment  
Distribution [[ ]] Note English units)

]]

Figure 4.8-8-4 Lower Tie Plate Seismic Test Fixture

[[

—

]]

Figure 4.8-8-5 Channel Clip Seismic Test Fixture

[[

]]

Figure 4.8-8-6 Channel [[ ]] Test Fixture

[[

]]

NRC RAI 4.8-9

*Section 4.2 of NEDC-33240P states, "Tests have been performed which show that significant interference between control blade and channels can be tolerated without causing a failure of the control blade to settle and without significantly affecting scram times."*

*(a) Provide the details of these tests.*

*(b) Recently, channel bow most likely due to shadow corrosion effects, has been a significant issue. Describe how channel bow and control blade interference will be managed for the GE14E fuel assembly design.*

GE Response

The primary control for channel-control blade interference is provided by the plant technical specifications surveillance where actions are specified both (1) to ensure control rod drive scram performance is consistent with requirements, and (2) to appropriately disposition instances where control rod operability, including channel-control blade interference effects, is less than adequate. With the ESBWR fine motion control rod drives, elevated channel-control blade friction approximately equivalent to [[

]] will enunciate a separation alarm as a result of control blade not settling – thereby positively identifying instances where an operability assessment is needed, and corresponding mitigating actions will be taken in accordance with the plant technical specifications. On this basis, no additional actions are required to assure plant safety.

Specific features of the ESBWR design, relative to currently operating BWRs, provide additional operating margin by minimizing the potential for elevated channel-control blade interference. For example, [[

]]

Additionally, the methodology presently applied to the operating BWRs to identify channel-control blade interference potential, as documented in Reference 4.8-9.1, will be similarly applied to ESBWR [[

]]

[[

]]

Reference

- 4.8-9.1 MFN 05-063, "Surveillance Program for Channel-Control Blade Interference",  
July 14, 2005.

NRC RAI 4.8-10

*Identify any deviations from the NRC-approved fuel mechanical design methodology (e.g. treatment of model uncertainties and manufacturing tolerances, rod power history, etc.) being employed in the evaluation of the GE14E fuel rod and fuel assembly design for ESBWR. Also, identify where the statistical methodology presented in Appendix A of NEDC-33242P has been previously reviewed and approved by the staff.*

GE Response

The methodology, including treatment of model uncertainties and manufacturing tolerances, is identical to that used to confirm compliance of the GE14 design with GESTAR for BWR/3-6 and ABWR (References 4.8-10.1 and 4.8-10.2). The licensing history of the fuel rod thermal-mechanical methodology is documented in the response to RAI 4.2-3.

References

- 4.8-10.1 Letter from C. O. Thomas (NRC) to J. S. Charnley (GE), 'Acceptance for Referencing of Licensing Topical Report NEDE-24011-P-A Amendment 7 to Revision 6, GE Standard Application for Reactor Fuel', March 1, 1985.
- 4.8-10.2 GE14 Compliance With Amendment 22 of NEDE-24011-P-A (GESTAR II), NEDC-32868P Revision 1, September 2000.

NRC RAI 4.8-11

*Demonstrate that the currently approved fuel performance models (e.g. models within GSTRM) are applicable to the GE14E design and ESBWR operating conditions (e.g. assembly average and nodal peak linear heat rate, power-to-flow ratio, etc.).*

GE Response

The lattice configuration, fuel rod design and fuel assembly design for the ESBWR are essentially identical to those employed in GE designed BWR plants currently operating in the United States and around the world. The only significant differences between the ESBWR GE14E fuel design and the standard GE14 design arise from the difference in the length of the fuel assembly. The GE14E design is ~30 inch shorter than the standard design to help accommodate a ~9m chimney above the fuel core. This chimney provides the driving head necessary to create and sustain the natural circulation flow for the ESBWR plant. This shorter assembly length results in shorter active fuel length and slightly different spacer pitch for some spans for the ESBWR design. Operating conditions for ESBWR, ABWR and BWR/3-6 plants are very similar except for reduced coolant flow for the ESBWR plant. Table 4.8-11-1 summarizes key operating conditions for the ESBWR and existing BWR plants.

**Table 4.8-11-1**  
**Reactor Operating Conditions**

Design Characteristics	ESBWR	ABWR	BWR/6
System operating pressure, Mpa	[[		
Core coolant flow rate, Mkg/h			
Coolant temperature, °C			]]

The GNF fuel rod thermal-mechanical performance model (GSTRM) has been extensively qualified and the results of the GSTRM (GESTR-Mechanical) experimental qualification have been previously provided to the USNRC (Reference 4.8-11.1 and 4.8-11.2). The pedigree of the GSTRM qualification and NRC approval is summarized in the response to RAI 4.2-3. Table 4.8-11-2 presents a summary of the experimental qualification database as compared to the GE14E fuel design characteristics.



**Table 4.8-11-2**  
**GSTRM Qualification Database**

Item	Fuel Temperature	Cladding Diametral Deformation	Cladding axial Deformation	Fission Gas Release	Rod Internal Pressure	GE14E
Number of Fuel Rods	[[					
Fuel Rod Diameter, in.						
Cladding Thickness, in.						
Diametral Gap, in.						
Pellet density, % TD						
Fuel Column length, in.						
He Pressurization, atm						
LHGR, kW/ft						
Rod Average Exposure, GWd/tU						]]

The comparisons in Tables 4.8-11-1 and 4.8-11-2 confirm that the GE14E design characteristics and ESBWR operating conditions are well within the GSTRM validation dataset. On this basis, it is concluded that GSTRM is directly applicable to GE14E licensing analysis.

#### References

- 4.8-11.1 J. S. Charnley, letter to R. Lobel, "Fuel Property and Performance Model Revisions", MFN- 170-84, December 14, 1984.
- 4.8-11.2 J. S. Charnley, letter to G. C. Lainas, "Fuel Property and Performance Model Revisions", MFN-027-086, April 7, 1986.

NRC RAI 4.8-12

*Section 3.3.1 of NEDC-33242P states, "The barrier concept has been demonstrated by experimental irradiation testing and extensive commercial reactor operation to be an effective preventive measure for PCI/SCC failure without imposing reactor operating restrictions." Provide the details of these power ramp tests including fuel rod design, fuel rod burnup, corrosion levels, and power history.*

GE Response

The GE14E fuel rod design includes a zirconium liner on the cladding inner surface. The barrier cladding concept was invented and implemented by GE/GNF to mitigate SCC/PCI failures. Prior to introduction of barrier fuel in reload quantities, barrier fuel was extensively tested under power ramp conditions in test reactors in a program sponsored by the US DOE. This testing convincingly demonstrated the high resistance of barrier fuel to duty-related failures. This experience is summarized in Reference 4.8-12.1.

The in-reactor performance of barrier cladding has confirmed the resistance of barrier fuel to duty-related failures within the normal operating domain. For example, to date, over [[ ]] GE11/13 fuel rods have operated at least 1 cycle and there have been no suspected duty-related failures. More recently, Severe Power Ramp testing has been performed to determine the failure threshold of barrier fuel at elevated exposures (Reference 4.8-12.2). The results from this Severe Power Ramp testing, as compared to the LHGR limits curves for recent and current GNF fuel designs, including GE14, are summarized in Figure 4.8-12-1. The apparent failure threshold based upon this recent testing is also indicated in Figure 4.8-12-1. This threshold is conservative in that it is a lower bound estimate based upon only failed rods; results for unfailed rods at powers significantly above the threshold are not shown. Even so, it is observed from Figure 4.8-12-1 that significant margin exists to the apparent failure threshold represented by the available ramp test results for operation without restriction below the LHGR limits for all designs, including GE14.

[[

]]

[[

]]

Figure 4.8-12-1  
LHGR Limits and Severe Ramp Test Failure Data

References

- 4.8-12.1 Fuel Ramp Tests in Support of a Barrier fuel Demonstration, GEAP-22076, Volumes 1 and 2, July 1984.
- 4.8-12.2 H. Sakurai, et. al., 'Irradiation Characteristics of High Burnup BWR Fuels', paper presented at the ANS Light Water Reactor Fuel Performance Conference held at Park City, Utah, April 10-13, 2000.

NRC RAI 4.8-13

*Section 3.4 of NEDC-33242P states, "The Zircaloy fatigue curve employed represents a statistical lower bound to the existing fatigue experimental measurements."*

*(a) Provide details on the supporting experimental data.*

*(b) Discuss the relative conservatism of GNF's fatigue data and methodology relative to the fatigue safety factors in SRP 4.2.II.A.1(b).*

GE Response

The data requested in (a) is summarized in Figure 4.8-13-1. The data comes from References 4.8-13.1 and 4.8-13.2. The nominal (mean) and lower 95/95 fatigue relations derived from the data are also indicated in Figure 4.8-13-1.

[[

]]

Figure 4.8-13-1  
Zircaloy Fatigue Curve

For fatigue analyses of structural members the guidance provided by SRP 4.2.II.A.1(b) is to either increase the amplitude by a factor of 2 or increase the number of cycles by a factor of 20. For cladding fatigue calculations, the assumed cyclic strain history includes [[

]] This very conservative cyclic strain history was derived to clearly bound the spectrum of actual anticipated operating conditions. With this conservative cyclic strain inventory, [[

]]

#### References

- 4.8-13.1 W.J. O'Donnell and Langer "Fatigue design Basis for Zircaloy Components". Nuclear Science and engineering: 20, 1-12(1964)
- 4.8-13.2 K. Petterson, "Low-Cycle Fatigue Properties of Zircaloy-2 Cladding," J. Nuclear Materials, 56(1975) 91.

NRC RAI 4.8-14

*Describe the treatment of the natural zirconium liner in each of the fuel rod analyses (e.g. assumed Zry-2, ignored, specific zirconium properties).*

GE Response

In the fuel rod analyses performed with the GSTRM model, the cladding is modeled as 2 layers (Zircaloy-2 and zirconium) and the liner is explicitly modeled and the impact of the liner on heat transfer and cladding strength are explicitly addressed. These analyses include the fuel temperature calculation, the cladding strain and fatigue calculations and the rod internal pressure calculation. In the calculation of the cladding critical pressure, which is performed to confirm that the rod internal pressure meets licensing requirements, the liner is [[ ]]

NRC RAI 4.8-15

*Table 4-1 of NEDC-33242P lists the parameters biased to their worst tolerance for the cladding strain analysis. Describe how the GSTRM model uncertainties (e.g. pellet thermal expansion, etc.) are accounted for in this evaluation.*

GE Response

As discussed in the response to RAI 4.8-16, the GSTRM fuel rod thermal-mechanical performance model (GESTR-Mechanical) has been qualified against experimental data that covers a wide range of not only duty conditions, but also dimensional conditions and fabrication parameters, to confirm the robustness of the embodied fundamental physical process and mechanism representations. The results of this qualification are used to define the model prediction uncertainty that is then explicitly included in the statistical fuel rod thermal-mechanical analyses. By the method of its derivation, this model uncertainty explicitly addresses uncertainties in material properties such as pellet thermal conductivity and thermal expansion, and cladding creep as well as uncertainties in submodels such as pellet relocation and pellet-cladding gap conductance. [[

]]

[[

]]

NRC RAI 4.8-16

*FRAPCON-3 benchmark cases appear to identify a difference in calculated fuel temperature relative to GSTRM. Please review the material presented in NUREG/CR-6534 Vol.4, Section 2 on burnup degradation of fuel thermal conductivity and the revised FRAPCON-3 thermal conductivity (ML051440720) and discuss the current conservatism within the GSTRM fuel thermal conductivity.*

GE Response

Qualification of the GSTRM fuel rod thermal-mechanical performance model (GESTR-Mechanical) was performed against an extensive and comprehensive fuel performance characterization data base in a manner to challenge the prediction capability over a wide range of duty conditions (power and exposure), dimensional conditions, and fabrication parameters to confirm the robustness of the embodied fundamental physical process and mechanism representations. [[

]]

The results of the GSTRM experimental qualification have been previously provided to the USNRC (e.g., References 4.8-16.1 and 4.8-16.2). For convenience, the fuel temperature qualification is reproduced here as Figures 4.8-16-1 through 4.8-16-2. Figures 4.8-16-1 and 4.8-16-2 demonstrate an excellent fuel temperature prediction capability that is unbiased both overall and as a function of exposure. [[



[[ ]]

Figure 4.8-16-1  
GESTR-Mechanical Fuel Temperature Qualification

]]

[[

]]

Figure 4.8-16-2  
Predicted/Measured Fuel Temperature as a Function of Exposure

Similarly, the cladding diametral deformation qualification database extends well beyond the linear heat generation rates and fuel exposures typical of commercial reactor operation, and again, the prediction capability is generally unbiased, although there is an observed tendency to overpredict cladding diametral deformation in some instances.

The GSTRM code has been used to calculate best estimate fuel centerline temperature and cladding permanent strain resulting from power ramps at the knee of the power-exposure LHGR limit curve for the GE14E UO<sub>2</sub> and [[ ]] w/o gad rods. The GSTRM results are presented in Table 4.8-16-1 as compared to corresponding FRAPCON-3 results for two cases representing (1)[[ ]], and (2)[[ ]].

These results could be applied, for example, for evaluation of an anticipated operational occurrence such as a pressurization transient. It should be noted that the GSTRM fuel thermal conductivity model does not include an explicit dependence on irradiation exposure (the fuel thermal conductivity is assumed to be exposure independent), whereas the FRAPCON-3 model includes an explicit exposure-dependent fuel thermal conductivity (decreases with increasing exposure).

[[



[[

]]

Figure 4.8-16-3  
PRIME Fuel Temperature Qualification

[[

]]

Figure 4.8-16-4  
Predicted/Measured Fuel Temperature as a Function of Exposure

Table 4.8-16-1 Code Comparison Results

**Thermal Overpower (TOP)**

	UO <sub>2</sub>			8 w/o Gd		
	T <sub>cl</sub> (start of TOP)	T <sub>cl</sub> (end of TOP)	T <sub>surface</sub> (end of TOP)	T <sub>cl</sub> (start of TOP)	T <sub>cl</sub> (end of TOP)	T <sub>surface</sub> (end of TOP)
GSTRM	[[					
PRIME						
FRAPCON						]]

	UO <sub>2</sub>			8 w/o Gd		
	EPS (start of TOP)	EPS (end of TOP)	Del(EPS)	EPS (start of TOP)	EPS (end of TOP)	del(EPS)
GSTRM	[[					
PRIME						
FRAPCON						]]

**Mechanical Overpower (MOP)**

	UO <sub>2</sub>			8 w/o Gd		
	T <sub>cl</sub> (start of MOP)	T <sub>cl</sub> (end of MOP)	T <sub>surface</sub> (end of MOP)	T <sub>cl</sub> (start of MOP)	T <sub>cl</sub> (end of MOP)	T <sub>surface</sub> (end of MOP)
GSTRM	[[					
PRIME						
FRAPCON						]]

	UO <sub>2</sub>			8 w/o Gd		
	EPS (start of MOP)	EPS (end of MOP)	del(EPS)	EPS (start of MOP)	EPS (end of MOP)	del(EPS)
GSTRM	[[					
PRIME						
FRAPCON						]]

Notes:

[[

]]

References

- 4.8-16.1 J.S. Charnley, letter to R. Lobel, "Fuel Property and Performance Model Revisions", MFN- 170-84, December 14, 1984.
- 4.8-16.2 J.S. Charnley, letter to G. C. Lainas, "Fuel Property and Performance Model Revisions", MFN-027-086, April 7, 1986.
- 4.8-16.3 The PRIME Model for Analysis of Fuel Rod Thermal – Mechanical Performance, Part 1 (Technical Bases), NEDC-22356P (in preparation).
- 4.8-16.4 P. Clifford (NRC), 'Re: GSTRM/FRAPCON comparisons', e-mail to R. Rand (GNF), July 18, 2006.